HUMAN DYNAMIC ORIENTATION MODEL APPLIED

TO MOTION SIMULATION

by

Joshua D. Borah

B.S., University of Colorado

(1972)

SUBMITTED IN PARTIAL FULFILLMENT

OF THE REQUIREMENTS FOR THE

DEGREE OF MASTER OF SCIENCE

at the

MASSACHUSETTS INSTITUTE OF TECHNOLOGY

June, 1976

Signature of Author_____

Department of Aeronautics and Astronautics
May 21, 1976

Certified by_____

Thesis Supervisor

Accepted by_____

Chairman, Departmental Graduate Committee

HUMAN DYNAMIC ORIENTATION MODEL APPLIED TO MOTION SIMULATION

by

Joshua D. Borah

Submitted to the Department of Aeronautics and Astronautics

on May 21, 1976, in partial fulfillment of the requirements

for the degree of Master of Science.

ABSTRACT

The Ormsby model of dynamic orientation, in the form of
a discrete time computer program, has been used to predict
non-visually induced sensations during an idealized coordi-
nated aircraft turn. It was found that attitude and angular
rate perceptions may be contradictory and furthermore, in a
three rotational degree of freedom simulator, it is impossible
to duplicate both simultaneously. To predict simulation fid-
elity, a simple scheme was devised using the Ormsby model to
assign penalties for incorrect attitude and angular rate per-
ceptions. With this scheme, it was determined that a three
rotational degree of freedom simulation should probably remain
faithful to attitude perception even at the expense of incor-
rect angular rate sensations. Implementing this strategy, a
simulation profile for the idealized turn was designed for a
Link GAT-1 trainer. Use of a simple optokinetic display was
proposed as an attempt to improve the fidelity of roll rate
sensations.

Two open loop subjective tasks were designed, to obtain
attitude and roll rate perception indications. A series of
experiments were performed in our modified Link trainer to
test the effectiveness of the tasks and to check model pre-
dictions and visual display effects.

The subjective responses were self consistent, and
both tasks are considered to be useful for obtaining low
frequency information. An unexpected difference was found
between subjective indications and model predictions for the
turn simulation. It can probably be explained by the response

lag inherent in the task (low bandwidth) plus consideration
of dynamic detection threshold effects; but this must be
clarified by further work. The optokinetic display was found
to be insufficient to significantly improve roll rate percep-
tion fidelity in the turn simulation, probably due to the
short duration of the movements involved.

Although not designed for the purpose, the predetermined
simulation profiles were rated for realism by two pilots. The
results did not contradict model predictions, although support
was weak. A dynamic simulator motion logic was proposed, in-
corporating the strategy derived from the model. Its use
would enable pilots to "fly" the simulator, and may provide
more convincing data for use in evaluating and revising the
fidelity prediction scheme.

Thesis Supervisor: Dr. Laurence R. Young
                     Professor of Aeronautics
                      and Astronautics

4

ACKNOWLEDGEMENTS

I wish to express my special gratitude to Professor Laurence R. Young for his patient guidance, encouragement, and support throughout this work.

I am also deeply indebted to Dr. Charles Ormsby, on whose work much of this thesis is based. Dr. Ormsby provided invaluable assistance to me in learning to understand and use his computer model and contributed many helpful suggestions as the work progressed.

In addition thanks go to Professor Renwick Curry for his help in the areas of psychophysical measurement and otpimal estimation theory; to Dr. John Tole, who patiently taught me to use the Lab computer system; to Mr. William Morrison, without whose help it would have been virtually impossible to keep all the necessary hardware in operation; and to Mrs. Sherry Modestino, who has been a tremendous aid in handling administrative chores and creating the final manuscript.

Finally, I wish to thank all the people at NASA Langley Research Center who went out of their way to assist me. Dr. M.J. Queijo and Mr. Ralph Stone, Jr. have continually encour-

aged and supported this project. Several people, among them Mr. Hugh Bergeron and Mr. Jacob Lichtenstein devoted significant amounts of their time to help me during one summer spent at the Langley facility.

TABLE OF CONTENTS

TABLE OF FIGURES

TABLES

SYMBOLS, ABBREVIATIONS, AND LABELS

α	angle of attack
α_a	absolute angle of attack
α	statistical significance criterion level
$\underline{A}$	acceleration vector
$\not\!AR$	aspect ratio
ADR-ADS	(see E)
ANAL1A	PDP-8 data reduction program used for analysis of roll rate estimation task, calibration runs
ANAL1B	PDP-8 data reduction program used for analysis of roll rate estimation task, simulation profile runs
ANAL2	PDP-8 data reduction program for analysis of vertical tracking task
β_0	linear regression intercept value
β_1	linear regression coefficient value
b_0	estimate of β_0
b_1	estimate of β_1
c_A	acceleration perception cost index
c_ω	angular rate perception cost index
c_γ	attitude perception cost index
CALn	Calibration profile n. Series of constant rate roll or pitch motions (see Figure 4.1)
DR	peak difference between subjective roll or pitch angle and subjective roll or pitch angle at the beginning of the stimulus period

DS	peak difference between Link pitch or roll angle and pitch or roll angle at the beginning of the stimulus period
<u>DOWN</u>	unit vector in the direction of earth vertical
E	error = (DR - DS)(sign of DS)
experiment 1	roll rate estimation task calibration (see Section 4.1)
experiment 2	subjective roll rate estimation during simulation profiles (see Section 4.2)
experiment 3	vertical tracking task during calibration profiles and simulation profiles (see Section 4.3)
$\underline{g}$	gravity vector
γ_b	angle between $\vec{i}_{zb}$ and <u>DOWN</u> where b is some particular reference frame.
$\hat{\gamma}$	angle between perceived <u>DOWN</u> ($\underline{\hat{DOWN}}$) and true <u>DOWN</u>
$\Delta\hat{\gamma}$	perceived deviation from upright
$\vec{i}_{xb}, \vec{i}_{yb}, \vec{i}_{zb}$	unit vectors along x, y, and z axes of some reference frame, b.
J	total perceptual cost index
lag factor	RLAG minus 1 second
p	roll rate (see Figure 2.2)
ϕ	roll angle (see Figure 2.2)
q	pitch rate (see Figure 2.2)
θ	pitch angle (see Figure 2.2)
r	yaw rate (see Figure 2.2)
ψ	yaw angle (see Figure 2.2)

RDUR	time from beginning of a stimulus period until DR reaches SVEL (seconds)
RESP	response
RESP'	subjective roll rate magnitude estimation response that has been transformed using the subject's calibration curve
RESP PK	peak subjective roll rate estimate during a given stimulus period (response scale divisions)
ρ	air density
$\rho_{x,y}$	coefficient of correlation between x and y
s	standard error of the estimate (regression analysis)
σ	standard deviation
SDUR	duration of non-zero Link roll or pitch rate during a stimulus period (seconds)
SET	a group of stimulus periods
SET PKG	set package. A group of sets entered as part of the data reduction PDP-8 programs
SPKGn	set package number n (see SET PKG)
SIM1	simulation profile found, using Ormsby model, to closely match attitude perceptions felt in a real aircraft during an idealized coordinated turn
SIM2	motion profile proportional to SIM1, but with roll magnitude twice as large
SIM3	coordinated turn simulation profile based on proportional roll strategy
STIM PK	peak Link roll rate during a given stimulus (°/sec)
SVEL	average Link pitch or roll rate during SDUR (°/sec)
stimulus period	segment of an experimental run for which certain stimulus and response parameters are calculated

SUBSCRIPTS

e   earth coordinates (see Figure 2.1)

hd   head coordinates (see Figure 2.1)

v   vehicle coordinates (see Figure 2.1)

s   sensor coordinates (see Figures 2.7 and 2.8)

av   aircraft vehicle coordinates

sv   simulator vehicle coordinates

cs   canal sensor coordinates

os   otolith sensor coordinates

xb, yb, zb   x, y, and z axes respectively in some coor-
               dinate frame, b.

CHAPTER I

INTRODUCTION

1.1   Basic Problem of Motion Simulation

It is often desirable to simulate the sensations of
riding in or operating some vehicle without using the vehicle
itself. Usually the device used for the simulation is much
more tightly constrained than the actual vehicle. The most
important example is probably that of aircraft simulation.
Whether training a pilot, evaluating handling characteristics
of a new aircraft, or trying out new instrument displays, it
is preferable to make initial tests without endangering a
pilot or an aircraft.

Modern aircraft simulators often have multi-degree of
freedom motion capabilities, but compared to an aircraft are
severely restricted by position, velocity, and acceleration
limits. A strategy must be devised for attenuating or "washing
out" the vehicle motions so that they fall within the simulator
constraints. The task, then, is to duplicate or approximate
the sensations produced by some motion history when only a much
more limited motion is available.

The motion parameters available to a person for use in
sensing motion are basically specific force and angular accel-
eration. These quantities can influence tactile sensors at
points of body contact with the vehicle, proprioceptive
sensors when muscles are stretched or compressed, and the
small inertial mechanism in the inner ear known as the vesti-
bular system. In a simulator, it is not possible to duplicate
all the specific force and angular acceleration profiles
attainable by the real aircraft. Often different degrees and
combinations of these vectors can be generated, sometimes one
to the exclusion of the other. For instance, it may be pos-
sible to duplicate the proper specific force direction only
at the expense of improper angular acceleration and vice versa.
A whole range of combinations varying between these extremes
is usually possible. It is not always obvious which strategy
will do the best job of making people feel as though they are
in the real aircraft.

1.2   Potential of Physiological Models

Very sophisticated washout designs have been developed,
especially since real time digital processing has become
feasible. Some state of the art motion logic designs for
multi-degree of freedom simulators can be found in the liter-
ature [7, 8, 21, 22, 24, 25]. Complex networks have been
developed for coordinating attitude and translational accel-
eration to obtain the desired specific force direction

without exceeding simulator constraints. The art has been extended by the use of non-linear adaptive filtering to present as much of a motion cue as possible [21].

Although physiological thresholds and sensitive frequencies are considered and are used in "tuning" these circuits, the basic attempt is still to minimize error in specific force and angular acceleration presentation. This has been the logical thing to do because these quantities have been the available, measurable parameters most closely related to motion perception. The human biological system, however, is not a perfect transducer of specific force or angular acceleration, and often does not even respond to these vectors in a linear fashion.

A physiological model, providing a reliable estimate of human perception during a given motion history, may be a very promising tool for simulation technology. Human perceptions in the simulator and aircraft could be objectively compared to gauge simulation fidelity, since it is the match up of overall perception that actually defines "realism".

1.3   Peripheral Vision Cues

This discussion has so far considered only the use of inertial motion to produce the feeling of movement. The feeling is also influenced by movement of the visual field. It seems that the peripheral visual field is especially important in

creating motion sensations, and can also effect perception
of spatial orientation. Almost everybody has, at one time
or another, experienced the illusion of moving by another
train in a railroad car only to discover themselves at
rest and the other train really the one in motion. The
same illusion can be created with a field of dots for exam-
ple, which move by as though the person is passing through
a tunnel with dotted walls. This phenomenon is called
visual linear vection [2, 33].

If the dot pattern moves in a circular fashion, as
though the person is rotating inside a cylinder with dotted
walls, a powerful illusion of rotational motion can be in-
duced and is called circularvection. If the circularvection
is about a horizontal axis, it may also induce a feeling of
tilt with respect to the vertical [9, 10, 33, 34).

These effects can be produced with many different visual
patterns and by using only the peripheral portion of the
visual field [2, 3, 33, 34]. An implication for aircraft
simulation, is that a relatively simple moving display on
the cockpit side windows may help create desired sensations.

1.4   Thesis Organization and Objectives

This thesis addresses only a very specific aspect of the
broad topics outlined in the preceding sections. In particu-
lar, it focusses on the problem of simulating aircraft coor-
dinated turns in a three degree of freedom Link GAT-1 trainer.

Coordinated turn dynamics are discussed in Section 2.1. A
model of "Human Dynamic Orientation" [20], based largely on
vestibular function, is used to predict the non-visually
induced sensations of a passenger during the maneuver.

The model has been adapted to provide a gauge of simu-
lation fidelity by using a simple, intuitively logical scheme
for assigning penalties to incorrect perceptions. Incorrect
perception is defined as any difference between perception
in the simulator and the aircraft. This penalty or cost
index analysis is then used to choose a motion profile for
the Link that is most likely the optimal simulation of a
particular turn. Sections 2.2 and 2.3 discuss the model and
its application to the turn problem. Section 2.4 examines
the possibility of augmenting the Link simulation derived in
2.3 by adding a moving horizontal stripe display on the cock-
pit windows. The current model does not account for visual
cues.

Chapter II, in summary, proposes a simulator motion pro-
file for a particular aircraft maneuver, presents estimates
of human perceptions in both the aircraft and simulation, and
describes a simple visual display that may aid the simulation.
The remainder of the thesis is devoted to experimental exami-
nation of material developed in Chapter II. The basic piece
of experimental equipment is a Link GAT-1 trainer modified to
interact with a hybrid computer. The equipment used is des-
cribed in detail in Chapter III. The questions addressed are

the following:

1. How well and how consistently can people
    dynamically indicate their attitude in a
    Link trainer?

2. During the turn simulation profile suggested
    in Chapter II, do people perceive the attitude
    history predicted by the model?

3. How well can people provide continuous
    dynamic estimates of their roll angular rate?

4. During the turn simulation profile, do people
    perceive and indicate the roll rate history
    predicted by the model?

5. Does a simple moving stripe display effect
    perception of either attitude or angular
    velocity during short duration roll motion?

6. Does the moving stripe display make perception
    of roll rate during a coordinated turn simula-
    tion more like model indications for the real
    turn?

7. How do pilots rate the "realism" of the turn
    simulation predicted as optimum by the model?

The data that has been gathered does not allow definitive
answers to all of these questions, but does shed some light.
Where a great deal of ambiguity still exists, the results do
suggest avenues for further investigation and represent a
first step as well as a good data base for further work.

CHAPTER II

ANALYSIS OF A COORDINATED TURN SIMULATION

2.1 Coordinated Turn Dynamics

In aircraft parlance, "coordinated" flight means
that the specific force vector remains vertical with
respect to the cockpit. When this is accomplished,
the pilot and passengers feel no side forces, only a
force of varying magnitude pushing them straight into
their seats. Most pilots, especially airline pilots,
always attempt to maintain coordination since their
passengers are most likely to feel more comfortable,
the coffee will not spill, etc.

For use in the physiological model and experiments,
a specific coordinated turn profile is needed. Most
convenient for this work is an idealized profile that
is as simple as possible while retaining the basic ele-
ments that make coordination difficult to simulate. This
is true for two reasons. The most compelling is that the
only way to get a completely realistic profile is to
record aircraft motions (attitude and accelerations) as
a pilot flies the maneuver, and such material is not

readily available. The second reason is that no two
pilots will roll in and out of turns with exactly the
same profile, and a single pilot will probably never
fly quite the same profile twice. It can, therefore,
be argued that more generalized conclusions can be
drawn by analysing an idealized situation.

Before proceeding further, some of the conventions
used in this thesis should be mentioned. Figure 2.1
specifies earth (e), vehicle (v) and head (hd) reference
frames. It will often be assumed that the head and air-
craft coordinates are parallel. Aircraft axes sometimes
appear in the literature with the z axis positive down
the the y axis through the right wing. The opposite has
been done here to make the system more compatible with
the physiological model discussed in the next section.
Figure 2.2 shows the convention used for pitch (θ), roll
(ϕ), and yaw (ψ) Euler angles, and was chosen to be com-
patible with the gimbal arrangement on the Link trainer
(described in section 3.1). Note that it is different
from the usual convention in which the order of pitch
and roll is reversed. Pitch, roll and yaw rates are
designated p, q, and r respectively. Specific force
(SF) is always taken as the gravity vector minus linear
acceleration with respect to the earth frame. Vector
quantities are underlined and unit vectors are capped
with arrows.

Figure 2.1   Earth, vehicle and head reference frames

Pitch

Roll

Yaw

Figure 2.2   Pitch, roll, and yaw angles

$xv''' \equiv$ North; $yv''' \equiv$ West; $zv''' \equiv$ Up

Figure 2.3 shows an aircraft during a turning maneuver. Assuming the turn is coordinated, airspeed is constant (thrust equals drag), and altitude is constant. Lift must balance gravity and impel the centripetal acceleration. Lift is always orthogonal to the velocity vector and $\vec{i}_{yv}$. Therefore

$$\phi_{SF} = \phi = \text{constant} \tag{2.1}$$

$$\omega = r = \text{constant} \tag{2.2}$$

$$L/M = SF = g/\cos\phi = \omega^2 R/\sin\phi \tag{2.3}$$

where L is lift. Rearranging 2.3

$$\omega = \frac{g}{\omega R}\tan\phi \tag{2.4}$$

Since ωR is airspeed (V), we can say that during a constant rate, constant altitude coordinated turn

$$r = (g/V)\tan\phi \tag{2.5}$$

The elevator and rudder apply torques about $\vec{i}_{yv}$ and $\vec{i}_{yz}$ respectively. By adjusting these controls, it is easy to see that the pilot can satisfy equation 2.5 while keeping horizontal angular velocity vectors zero.

When flying straight and level, lift just balances gravity. To achieve a constant altitude coordinated turn, this lift per unit mass must be multiplied by a

Figure 2.3 Aircraft during turn maneuver . The craft is shown flying
into the page, therefore the bank angle (φ) is negative.

factor of $1/\cos\phi$ (equation 2.3). The pilot can do this in several ways, the easiest being to increase the angle of attack slightly. Since drag as well as lift will increase, airspeed will be somewhat slower during the turn. The original airspeed can be maintained, however, by increasing power during roll-in.

The change in pitch angle is often very small. Let us look at the case of a Cessna 150 performing a coordinated turn. A cessna 150 has been chosen for the example because the Link trainer used in this work is built to simulate a small single engine aircraft. Let us consider the aircraft to be cruising straight and level at 85 knots (a typical cruise speed for this plane) and 10,000 feet, when it enters a 30 degree bank coordinated turn. This is a steep turn and can be considered a fairly extreme case, although not unusual. Also assume that the pilot maintains airspeed and altitude and that all lift is applied by the wings. At 10,000 feet, air density (ρ) is 0.001756 slugs/ft^3, Cessna 150 wing area (S) is 157 ft^2, and gross weight is 1000 pounds [29]. Assuming two 150 pound occupants, wing coefficient of lift (C_L) before entering the turn can be calculated.

$$C_L' = L'/\tfrac{1}{2}\rho V^2 S \simeq 0.46 \qquad (2.6)$$

Once in the constant turn, wing coefficient of lift is

$$C_L'' = L''/\tfrac{1}{2}\rho V^2 S \qquad\qquad (2.7)$$

Substituting V^2 from equation 2.6 and noting that L' is Mg and L" is Mg/cos 30°,

$$C_L'' = C_L'/\cos 30° \qquad\qquad (2.8)$$

$$\Delta C_L = C_L'(1/(\cos 30°) - 1) \simeq 0.07 \qquad (2.9)$$

For a thin airfoil (infinite aspect ratio) the slope of the lift curve is

$$m_0 = \Delta C_L/\Delta a = 2\pi \qquad\qquad (2.10)$$

$$a \equiv \text{angle of attack}$$

Assuming an elliptical lift distribution, a finite wing has a lift curve slope

$$m = \Delta C_L/\Delta a_a$$

$$= (m_0/(1 + m_0)/\pi AR \qquad [16] \quad (2.11)$$

$$AR = \text{aspect ratio}$$

$$a_a = \text{absolute angle of attack}$$

The Cessna 150 has an aspect ratio of 6.7 giving an m of 4.84. This yields a $\Delta\alpha_a$ of .0145 radians or .83 degrees. In other words, the pitch change in question is about one degree.

Of course a real pilot cannot manipulate controls precisely enough to maintain perfect coordination and airspeed. Other transient disturbances will be introduced by relative flow velocity perpendicular to wing and tail fin surfaces during roll. The important point to note, however, and the element that makes this maneuver a simulation problem, is that the specific force vector rolls with the cockpit and increases in length. It may deviate slightly from cockpit vertical now and again, but to an observer in the craft it does not indicate cockpit roll angle or roll rate. In a three degree of freedom device, with only pitch, roll, and yaw motion available, it is not possible to create this situation. Even in a multi-degree-of-freedom simulator, with lateral motion capability, it is not possible to sustain a roll angle very long without allowing specific force to realign with earth vertical. It is this aspect of the turn that should be emphasized in the idealized version to be analyzed with the physiological model.

The basic parameters selected for the idealized turn are those used in the Cessna 150 example: a 30 degree bank, 85 knot, constant altitude, coordinated turn, maintaining airspeed during roll-in and roll-out. This will yield a turn rate of about 7 degrees per second, considerably faster than the

standard 3 degree per second turn; but it is by no means
unreasonable and the steep bank angle will emphasize the
affects of coordination. A typical roll rate in a small
plane is about 10°/second. The roll profile used here is
shown in Figure 2.4 and is essentially a constant roll rate
during roll in and out with tenth second ramps leading to and
from the constant value. There is no doubt that a real pilot
does not maintain a constant rate, but probably increases to
a maximum and decreases back to zero in a more or less smooth
curve. Without actually measuring this in the real situation,
there is no telling whether a typical profile is fit more
closely by a square wave, a trapezoid, a triangle, a sinusoid,
etc. The profile of Figure 4.2 was chosen as the simplest.

The yaw rate profile, also shown in Figure 2.4, satisfies
equation 2.5. The pitch angle change necessary in the real
maneuver is quite small compared to other events. The precise
profile will again depend on the pilot, and will probably be
the same order of magnitude as the disturbances associated
with imperfect attempts to maintain coordination and airspeed.
It does not present a simulation washout problem since the
pitch change is reflected in a change of specific force
direction. Finally, it will be seen later that one degree of
pitch is below the resolution of the psychophysical estimates
obtained for this work. All these things, considered, it
makes sense to simply ignore this small pitch adjustment and
assume lift magically increases by the desired amount.

Figure 2.4   Idealized coordinated turn profile

For convenience $\vec{i}_{xv}$ is assumed to be horizontal at the cruise angle of attack, and specific force is modelled as remaining parallel to $\vec{i}_{zv}$ with a magnitude satisfying equation 2.3. The motion profile described by Figure 2.4 and the above three paragraphs is the turn analysed in the remainder of the thesis.

2.2   Ormsby Model of Human Dynamic Orientation

A model for predicting perceptual responses to motion stimuli has been developed at the MIT Man-Vehicle Laboratory by Charles Ormsby [21]. The model is based on the known mechanics of the vestibular organs. It assumes an optimal processing strategy by higher centers to obtain estimates of attitude and motion and was designed to be consistent with available neurophysiological and psychophysical data. Since much of this data is derived from experiments which necessarily include tactile and proprioceptive motion cues, it can be argued that the model is tuned to account for some of these cues. It must be regarded, however, as primarily a vestibular information and information processing model.

The vestibular system is composed of two types of sensors. The rotational motion sensor is a set of three roughly orthoganol toroids, or circular canals. The canals are fluid filled and completely obstructed in one section by a gelatinous mass called the cupula. Imbedded in the cupula are hair cells which can respond to deformation in one sensitive direction.

When a canal is accelerated about its axis of symmetry, the
endolymph fluid lags behind the canal walls and applies a
force to the cupula. The resulting deformation is trans-
formed to an afferent firing rate and signals a rotational
motion. A set of these organs, called semicircular canals,
are contained in the membranous ducts within bony, fluid
filled labyrinths on either side of the head, behind the
auditory portion of the ear.

The other type of sensor, responsible for detection of
specific force, is a gelatinous mass containing calcium car-
bonate crystals (otoconia) and supported by a bed of hair
cells (maculae). This structure is also immersed in a fluid
(endolymph), but since the otoconia are denser than the
fluid, a change in specific force will cause them to move
relative to the labyrinth thus deforming the supporting hair
cells. On each side of the head, occupying the same labyrin-
thine structure as the canals, are two such organs: the
utricular and saccular otoliths. The utricular sac actually
serves as both the housing for the utricular otolith and the
base reservoir of the three canals.

Orientation of the canals and otoliths is shown schemat-
ically in Figures 2.5 and 2.6. Each canal is excited (affer-
ents increase their firing rate over resting levels) by angular
acceleration in one direction along its sensitive axis, and
is asymmetrically inhibited by rotation in the opposite direc-
tion. Since the two canal sets behave with opposite polarities,

Figure 2.5   Orientations and polarizations of the semicircular canals

(from Ormsby (21))

UTRICLES

SACCULES

Figure 2.6   Orientation of Otoliths

(from Ormsby (21))

a sort of push-pull system is created yielding a roughly symmetric combined response. The utricular macula contains hair cells of all orientations and is sensitive in all directions parallel to its plane. The saccule is predominantly sensitive in the direction perpendicular to the average utricular plane. The system is described in much greater detail in references 15, 18, 21, and 32.

For modelling purposes the system is simplified to one cyclopian system consisting of three canal and three otolith organs. All organs are modelled as responding symmetrically along their sensitive axes which are shown in Figure 2.7 and 2.8. These axes will be referred to as otolith and canal sensor coordinates. The response of each canal along its sensitive axis is modelled as a highly overdamped torsion pendulum, with an added rate sensitivity and adaptation term presumably due to afferent processing. Although actually an angular acceleration sensor, the excess damping quality causes a response that is proportional to angular velocity for high frequencies. Indeed, the system seems to interpret canal responses as angular velocity. The model assumes, for each canal, the following transfer function for afferent response to angular acceleration.

$$
\underbrace{\frac{FR_{cs}(s)}{\omega(s)} = (573) \underbrace{\frac{s}{(18s+1)(0.005s+1)}}_{\text{torsion pendulum}} \underbrace{\frac{30s}{(30s+1)}}_{\text{adaptation}} \underbrace{(0.01s+1)}_{\substack{\text{rate} \\ \text{sensitivity}}}}_{} \tag{2.12}
$$

$$
FR_{cs}(s) = \text{(canal afferent firing rate)}
$$

Canal coordinates $\equiv$ (xc, yc, zc)

Otolith coordinates $\equiv$ (xo, yo, zo)

Figure 2.7   Cyclopian sensor coordinates

Figure 2.8   Sensitivity of cyclopian canal system

(from Ormsby (21))

44

ω(s) =   (angular velocity along sensitive axis)

(spontaneous firing rate neglected)

The otoliths are modelled as linear accelerometers with an added rate sensitivity term due either to mechanical properties or possibly afferent processing. The afferent dynamic response to specific force is taken as follows:

$$\frac{FR_{os}(s)}{SF(s)} = (18000) \underbrace{\frac{1}{(s + 0.2)(s + 200)}}_{\text{accelerometer}} \underbrace{(s + 0.1)}_{\substack{\text{rate} \\ \text{sensitivity}}} \qquad (2.13)$$

FR_{os}(s) =   (otolith afferent firing rate)

SF(s) =   (specific force along sensitive axis)

Detailed derivations for equations 2.12 and 2.13 can be found in chapters two and three of Ormsby's thesis [21].

Inputs to the Ormsby model are time histories of specific force and angular velocity vectors given in head coordinates ($\underline{SF}_{hd}$(t) and $\underline{\omega}_{hd}$(t)). The first step in implementing the model is transformation of these inputs to sensor coordinate axes. It is then assumed that these afferent responses are the signals available to the human nervous system processing mechanism. From this point on the model becomes very phenomenological since we do not yet approach a capability to deduce central processing algorithms from central nervous system wiring. It is assumed that central processors do something akin to a least mean squares error optimization to estimate specific force and angular velocity inputs based on afferent output. If the system has no a priori information about input

besides an expected magnitude range and frequency bandwidth
(mathematically described as a Markov process), and also
expects a certain amount of measurement noise, the least
mean squared error estimator is a Kalman filter. If input
and measurement noise statistics are time invariant, this
reduces to a steady state Kalman (or Wiener) filter. It is
a steady state Kalman filter that is implemented by the model
and tuned to yield $\hat{\underline{SF}}_{os}$ and $\hat{\underline{\omega}}_{cs}$ estimates to fit available
data. (The hat above the two terms signifies that they are
perceptual estimates and the subscripts identify them as
otolith and canal estimates respectively.)

In the case of the canals, the filter is "tuned" so
that estimates of $\hat{\underline{\omega}}_{cs}$ are essentially the same as afferent
responses. This reflects available perceptual and neuro-
physiological data, and suggests that little central proces-
sing is required. The otolith filters, however, have a more
dramatic effect on specific force estimates in order to fit
perceptual data. This suggests either a significant amount
of central processing or that a term which should be present
in the afferent model is being attributed to the higher cen-
ters. The basic effect of the otolith Kalman estimator is
to low pass filter the afferent signal with a time constant
of about 0.7 seconds. The only difference between utricle
and saccule filters is the gain, the saccule gain being half
that of the utricle.

At this point, the model has generated estimates of
three specific force components and three angular velocity
components. The saccule component is transformed by a non-
linear input-output function, one way to account for observed
attitude perception inaccuracies known as Aubert or Mueller
[13] effects, and the resulting estimates are transformed
back to head coordinates. These two vectors $(\hat{\underline{SF}}_{hd}(t)$ and
$\hat{\underline{\omega}}_{hd}(t))$ must now be combined to yield an overall estimate of
attitude, linear acceleration and angular acceleration.

The basic premise for the next operation is that the
system will depend most heavily on the otolith specific force
estimate for low frequency attitude information, and will
look to the canals to find out about high frequency attitude
changes. Figure 2.9 diagrams this logic. Block A computes
the rotation rate of $\hat{\underline{SF}}_{hd}$. Block D separates $\hat{\underline{\omega}}_{hd}$ into parts
agreeing with $\hat{\underline{\omega}}_{SF}^{H}$ (called $\hat{\underline{\omega}}_{c}^{c}$) and parts contradicting $\hat{\underline{\omega}}_{SF}^{H}$
(called $\hat{\underline{\omega}}_{c}^{i}$). All other operations are clear from the diagram.
The output of Figure 2.9 is labeled $\hat{\underline{DOWN}}$ and is a vector of
length 1 g, in the direction of perceived vertical. The $\hat{\underline{DOWN}}$
vector is the model's prediction of attitude perception.
Linear acceleration perception is assumed to be $\hat{\underline{DOWN}} - \hat{\underline{SF}}_{hd}$.

Perception of angular velocity parallel to $\hat{\underline{DOWN}}$ is simply
the component of the canal estimate parallel to $\hat{\underline{DOWN}}$. Angular
velocity perpendicular to $\hat{\underline{DOWN}}$ is the derivative of $\hat{\underline{DOWN}}$ $(\dot{\underline{D}})$
plus the high pass portion of any canal signal both perpendi-
cular to $\hat{\underline{DOWN}}$ and not present in $\dot{\underline{D}}$. This is diagrammed in

Figure 2.9 $\widehat{\text{DOWN}}$ Estimator (From Ormsby [21])

Figure 2.10 $\underline{\omega}$ Estimator (from Ormsby, reference 21)

Figure 2.10.   A much more detailed explanation of Figures 2.9 and 2.10 can be found in Chapter 8 of Ormsby's thesis [21].   Figure 2.11 schematically summarizes the entire model.

It should be pointed out that the preceding description relates only to the particular model used in this thesis.   Ormsby also made provision for spontaneous firing rate and random measurement noise input.   With these features, Monte Carlo simulations can be set up and threshold phenomenon studied.

It should be noted that the inputs $\underline{SF}$ and $\underline{\omega}$ must act on the body as a whole and derive from an outside source.   Voluntary head movements are likely to involve corollary discharge of one sort or another, possibly to vestibular organs themselves and certainly to central processors telling them what to expect.   This constitutes a new situation.   The caution is not meant to imply that the model cannot be useful in studying voluntary movements, but only that it cannot be used simply as a black box to predict perceptions under such conditions.   Consideration of pilots who are controlling their craft presents somewhat less of a problem, since they are acting indirectly through the vehicle.   Nonetheless, they certainly have prior knowledge, or expectation of the motion, and this must be kept firmly in mind whenever the model is applied to them.

Figure 2.11   Schematic of Ormsby model.   DOWN and ω estimators are shown in Figures 2.9 and 2.10 respectively.

51

The model is used in the form of a digital FORTRAN IV program. In the version used for the work of this thesis, afferent responses (equations 2.12 and 2.13) are updated every 0.1 seconds and Kalman filter estimates are updated every second. An annotated listing of the program with instructions for use appears in Appendix A.

2.3 Model Predictions for the Coordinated Turn

In order to apply the Ormsby model to the coordinated turn of section 2.1, let us assume that the aircraft roll axis passes directly through the origin of the occupant's head axis system. We shall also assume that the vehicle and head coordinate axes always remain parallel. The first and most obvious observation is that canal and otolith responses will be contradictory. Since specific force remains in the same direction with respect to the subject, otoliths indicate no change in roll attitude. Canals, on the other hand, are sensitive to the angular velocity produced by roll-in. Looking at Figure 2.9, it can easily be seen that the only non-zero signal travels the upper loop through blocks D, E, and F.

A quick idea of what to expect can be obtained
by reducing the model to blocks E, F, and G of Figure
2.9. This is shown in Figure 2.12. Blocks H and I
are dropped since they will only come into play if
integration errors accumulate. Over the three seconds
of roll-in, equation 2.12 will yield a response that
is roughly proportional to the input. Figure 2.12
then, leads us to expect a roll attitude perception
that looks very much like the roll rate stimulus
profile.

Although the specific force vector has not
rotated, it has elongated and therefore brings into
play the saccule nonlinearity mentioned in section
2.2. The expected result is an "elevator illusion" of
being tilted backwards. A component of r along $\vec{i}_{yhd}$
also contributes to the tilt illusion. Figure 2.13
shows the actual predictions of the computer model
for roll and pitch attitude perception during the
roll-in phase of the idealized coordinated turn.

Now we come to the perception of angular rate.
If r_L in Figure 2.10 is 0, it can be seen that roll

E

$$\frac{s}{\tau_E s+1}$$

F

$$1$$

G

$$\frac{1}{s}$$

ω_{xhd}

roll
attitude
perception

Further reduces to:

$$\frac{1}{\tau_E s+1}$$

ω_{xhd}

roll attitude perception $(\hat{\phi})$

$(\tau_E \simeq 0.25$ seconds$)$

Figure 2.12 $\underline{\text{DO}\hat{\text{WN}}}$ estimator reduced to approximate roll attitude during
coordinated turn. Block G has been simplified to keep track
of $\hat{\phi}$ instead of rotating the $\underline{\text{DO}\hat{\text{WN}}}$ vector. Block F is unity
because there is only one component $\omega^i_{c_{xhd}}$ which in this case
is approximately perpendicular to
$\underline{\text{DO}\hat{\text{WN}}}$.

rate perception is just the derivative of roll attitude. If, on the other hand, τ_L is large, Figure 2.10 says the system will "trust" the canals and will perceive a roll rate more nearly following the roll velocity stimulus. Note that this roll rate perception will be inconsistant with the roll attitude perception shown in Figure 2.13. The hypothetical person feels a roll rate that is larger than the derivative of his attitude estimate. Contradictory sensations of a similar nature are well documented for other situations. One such example is that of visual circularvection about a horizontal axis and is mentioned in the introduction (section 1.3). There is a whole range of possible responses between the two examples given depending on the value of τ_L, and the proper value for τ_L is not at all clear. Ormsby makes a claim for a value between 0 and 5 seconds [21]. Figure 2.14 shows the model predictions for angular rate perception during roll in using both $\tau_L = 0$ and $\tau_L = 5$ seconds.

It should be assumed that Figures 2.13 and 2.14 represent a naive subject. A pilot has prior knowledge of the maneuver having initiated it, and has usually experienced the profile many times before. It is possible that his innate feelings are the same as those of a naive passenger, but are interpreted

Figure 2.13 Model predictions for roll and pitch perception during initiation of the idealized coordinated turn. The idealized turn profile is shown in figure 2.4.

Figure 2.14 . Model predictions for roll and pitch perception during initiation of the idealized coordinated turn. The idealized turn profile is shown in figure 2.4.

differently. It is also conceivable that mental set
causes the pilot to experience sensations that are
actually different from those of the naive person. For
example, the pilot may turn up his τ_E value (in Figure
2.9) having learned that canal estimates are all he has
to go on. If τ_E is large, a person will "trust" his
canals and in this case will not be far wrong in esti-
mating roll angle during roll-in. As the turn continues
at constant bank angle, blocks H and I of Figure 2.9,
which must now be considered, will cause attitude per-
ception to gradually realign with $\hat{SF}$. The human nervous
system is amazingly plastic and the above is one of many
possible conjectures that can only be verified experi-
mentally. Finally, remember that figures 2.13 and 2.14
represent non-visually induced sensations.

Although several cautions and uncertainties have
been mentioned, it is highly likely that the gross pre-
dictions of the model are correct. During a coordinated
turn, people will feel only a small change in roll atti-
tude compared to their true roll, a roll rate that may
be somewhat more pronounced, and a slight pitch back
sensation as specific force increases.

2.4   Simulation Fidelity Analysis

If we assume that the Ormsby model is giving a
meaningful estimate of human perceptions, it should
be useful in gauging the effectiveness of a given sim-
ulation. It makes sense to look at some function of
the difference at each sampling instant, between model
outputs for the real motion and the simulator motions.
These outputs are $\underline{\hat{DOWN}}$ (attitude perception vector),
$\underline{\hat{\omega}}_{hd}$ (angular velocity perception vector), and an ac-
celeration perception vector ($\underline{\hat{A}}$) equal to

$$\underline{\hat{DOWN}} - \underline{\hat{SF}}$$

The function sought should be dimensionless and should
be proportional to the cost in "realism" of any per-
ceptual error. There is currently no data available
to indicate the quantitative loss in realism ascribed
by humans to a given difference in perceptions.

It seems logical, therefore, to pick as a cost
index the simplest function that makes intuitive sense.
When sensations are clearly suprathreshold, the most

likely candidate is just percent error, the ratio
of perceptual error to the correct quantity. The
computer model in the form being used here does
not account for perceptual thresholds, and when
sensations are in the subthreshold region, the in-
tuitive sense of the above scheme breaks down. It
does not seem reasonable to assess a heaby penalty
to an error when all quantities are probably below
threshold. When the model indications for "correct"
perceptions are subthreshold it seems more reasonable
to assess a large penalty for errors that are large
compared to the threshold value. Costs for each of
the model outputs have been computed as follows:

$$\Delta\hat{\omega}(t) = \left| \hat{\underline{\omega}}_{av}(t) - \hat{\underline{\omega}}_{sv}(t) \right|$$

$$\Delta\hat{A}(t) = \left| \hat{\underline{A}}_{av}(t) - \hat{\underline{A}}_{sv}(t) \right| \qquad (2.14)$$

$$\Delta\hat{\gamma}(t) = \text{angle between } \underline{\hat{DOWN}}_{av} \text{ and } \underline{\hat{DOWN}}_{sv}$$

Subscripts: sv $\equiv$ simulator vehicle

av $\equiv$ aircraft vehicle

$$C_\omega(t) = \begin{cases} \dfrac{\Delta\hat{\omega}(t)}{|\hat{\underline{\omega}}_{av}(t)|} & \text{for} \quad |\hat{\underline{\omega}}_{av}(t)| > \hat{\omega}_{thr} \\[2em] \dfrac{\Delta\hat{\omega}(t)}{\hat{\omega}_{thr}} & \text{for} \quad |\hat{\underline{\omega}}_{av}(t)| < \hat{\omega}_{thr} \end{cases}$$

$$C_A(t) = \begin{cases} \dfrac{\Delta\hat{A}(t)}{\hat{A}_{av}(t)} & \text{for} \quad |\hat{\underline{A}}_{av}| > \hat{A}_{thr} \\[2em] \dfrac{\Delta\hat{A}(t)}{\hat{A}_{thr}} & \text{for} \quad |\hat{A}_{av}| < \hat{A}_{thr} \end{cases}$$

$$C_\gamma(t) = \begin{cases} \dfrac{\Delta\hat{\gamma}(t)}{|\hat{\gamma}_{av}(t)|} & \text{for} \quad |\hat{\gamma}_{av}| > \hat{\gamma}_{thr} \\[2em] \dfrac{\Delta\hat{\gamma}(t)}{\gamma_{thr}} & \text{for} \quad |\hat{\gamma}_{av}| < \hat{\gamma}_{thr} \end{cases}$$

subscript: thr ≡ perceptual threshold

The individual costs indices ($C_A(t)$, $C_\omega(t)$, and $C_\gamma(t)$) are simply weighted and summed to form an overall index.

$$J(t) = C_A(t) + C_\omega(t) + C_\gamma(t) \tag{2.15}$$

No attempt is made here to mathematically minimize J. It is presented only as a simple index for comparing given simulations and, of course, can be used to pick the choice with the lowest index from among several possibilities.

For the case of the Link simulation, it is fairly easy to see what will happen once several things are realized. In the Link, which is capable only of pitch, roll and yaw motion, specific force will always line up with gravity except during transient roll and pitch accelerations (the occupant's head

is above the roll and pitch axes). This is the situation that the vestibular system has evolved to handle and will not produce serious disagreement between the canals and otoliths. The only possible exceptions may occur if a person is subjected to large, sustained yaw rates creating the possibility of Coriolis illusions, or sustained "barbeque spit" type motions causing the otoliths to signal a rotating specific force vector long after canal signals have attenuated to zero. Barbeque spit motion is not possible in the Link (pitch and roll are restricted to less than 20 degrees in either direction) and yaw will be too slow during the turn maneuver to create Coriolis problems. Therefore, we can expect the Ormsby model to predict roughly accurate perceptions of roll and pitch attitude and angular rates.

The next thing to notice is that absolutely nothing can be done towards creating the model's linear acceleration perception which is in the $\vec{i}_{zhd}$ direction and quite small anyway. This leaves us with the problem of minimizing the last two terms of J (equation 2.15). Let us first consider only roll motion and momentarily neglect pitch and the component of $\underline{\omega}$ parallel to DOWN. If equation 2.15 is reduced to only roll considerations

$$J' = \beta_\gamma \left| \frac{\hat{\phi}_{av} - \hat{\phi}_{sv}}{\hat{\phi}_{av}} \right| + \beta_\omega \left| \frac{\hat{p}_{av} - \hat{p}_{sv}}{\hat{p}_{av}} \right| \qquad (2.16)$$

$\hat{\phi} \equiv$ roll angle perception; $\hat{p} \equiv$ roll rate perception

The first term can be zeroed approximately by following the figure 2.13$\hat{\phi}_{av}$ profile with the Link Trainer. Remember, in the Link as opposed to the aircraft, roll rate sensation will be the derivative of roll attitude sensation regardless of τ_L.

$$\hat{\phi}_{sv}(t) = d\hat{\phi}_{sv}(t)/dt \qquad (2.17)$$

If $\tau_L = 0$, equation 2.17 holds for the aircraft also, and both terms of equation 2.16 have been zeroed. Both $\hat{\phi}_{sv}$ and $\hat{\phi}_{av}$ will follow the open circles in figure 2.14. If $\tau_L = 5$ secs, $\hat{p}_{av}$ is represented by the solid circles in figure 2.14, while $\hat{p}_{sv}$ follows the open circles. Since $\hat{\phi}_{sv}$ is the integral of $\hat{p}_{sv}$, it can easily be seen that with $\beta_\omega/\beta_\gamma = 1$, any change in simulator motion decreasing the second term of 2.16 will quickly be overbalanced by an increase in the first. Unless $\beta_\omega/\beta_\gamma$ is much greater than 1, J' is minimized for this case by remaining faithful to roll attitude perception. There is no reason to believe that angular rate perception should be weighted more heavily than attitude perception. Although this is all somewhat hypothetical, the conclusion is that the most likely candidate for "optimal simulation" will recreate roll attitude perception.

If we now consider pitch motion, the same argument will lead to the conclusion that pitch attitude perception should be duplicated at the expense, if necessary, of pitch rate perception. A good first try at duplicating pitch attitude perception is to follow, with Link motion, the figure 2.13

pitch curve to its maximum, sustain that value through the constant phase of the turn, then pitch-out with a mirror image of pitch-in.

We have so far considered everything but angular rate perception about $\vec{i}_{zhd}$. This can be closely duplicated by adjusting Link yaw velocity to produce an $\vec{i}_{zhd}$ component equal to that in the aircraft. In other words, satisfy

$$r_{sv} \cos \gamma_{sv} = r_{av} \cos \gamma_{uv}$$

$$r_{sv} = r_{av} \frac{\cos \gamma_{av}}{\cos \gamma_{sv}}$$

(2.18)

$\gamma_{sv} \equiv$ total angle between simulator
zv axis and vertical

$\gamma_{av} \equiv$ total angle between aircraft
zv axis and vertical

Figure 2.15 shows a coordinated turn simulation profile for the Link trainer based on the above arguments. Model predictions for motion perception during this profile are shown in figures 2.16 and 2.17. Model predictions for the aircraft turn (assuming $\tau_L = 5$) have been superimposed. According to the model, proper attitude perception has been virtually duplicated although there has been some expense to pitch and roll angular rate perception as anticipated. Angular rate perception about $\vec{i}_{zhd}$ has also been closely duplicated. Figure 2.18 shows the results of cost index calculations for the simulation of figure 2.15. Weighting factors have been taken as 1, and τ_L has been taken as 5 seconds. Figure 2.19 shows the case of zero τ_L. The

Figure 2.15 A coordinated turn simulation profile for the Link trainer

roll orientation perception during idealized aircraft turn

roll orientation perception during simulation

pitch orientation perception during idealized aircraft turn

pitch orientation perception during simulation

Figure 2.16 Pitch and roll rate perceptions during a simulation of the idealized coordinated turn. (The idealized turn profile is shown in figure 2.4 and the simulation profile is shown in figure 2.15.)

Figure 2.17 Pitch and roll perception during a simulation of the idealized coordinated turn. The idealized turn profile is shown in Figure 2.4 and the simulation profile is shown in Figure 2.15.

cost, or fidelity index program that implements these calculations is listed in Appendix A. When flown with its own "factory" logic, the Link GAT-1 trainer employs a proportional roll and over a certain range, maintains roughly 1/6 of the imaginary aircraft roll angle. Aircraft yaw rate is reproduced exactly. When a motion history based on this logic is input to the fidelity index program, the results are as shown in Figure 2.20.

COST

● total cost (J)

⅄ acceleration perception cost (C_A)

□ angular velocity perception cost (C_ω)

○ attitude perception cost (C_γ)

Figure 2.18 Cost computation for simulation profile shown in Figure 2.15 assuming $\tau_L = 5.0$.

t (sec)

Figure 2.19   Cost computation for simulation profile shown in Figure 2.15 assuming $\tau_L = 0$.

● total cost (J)

▲ acceleration perception cost (C_A)

□ angular velocity perception cost (C_ω)

○ attitude perception cost (C_γ)

Figure 2.20 Cost computation for simulation profile based on proportional roll strategy.

2.5   Use of the Circularvection Display

Our modified Link trainer is outfitted with a
visual display system capable of projecting moving
horizontal stripes on the translucent, cockpit side
windows. It is described in greater detail in sec-
tion 3.2. When τ_L is greater than zero, section
2.4 predicts an angular velocity sensation, during
coordinated turn roll-in and roll-out, that simply
cannot be generated by Link trainer motion without
producing a grossly incorrect attitude perception.
Perhaps this "missing" velocity sensation, or a part
of it, can be produced visually.

The Link stripes can be made to move up on one
window and down on the other, producing an opto-
kinetic roll display. It has been shown that this
display can produce the paradoxical illusion of con-
stant tilt with respect to vertical. Dichgans, Held,
Young and Brandt [10] measured this tilt illusion (in
the same Link trainer used for this work and
using a very similar visual display). They found that

subjects instructed to maintain an upright orientation (the subject was able to control Link roll motion with a control stick) tilted themselves an average of 8.5 degrees in the direction of stripe motion. Stripe speed was varied between 14 and 26 degrees per second and tilt reached steady state after an average of 17 sec. Onset time for the constant roll velocity sensation was not measured. Experiments using a much larger visual field display have produced tilt deviations up to at least 45 degrees [35]. Although the latter experiment was performed at varying head tilt angles, as was an experiment by Dichgans, Diener, and Brandt [9], it has never been tried during actual rolling motions. Young, Dichgans, Murphy and Brandt [33] have performed an experiment, also in the Man-Vehicle Lab Link trainer, in which yaw angular velocity was combined with a yaw optokinetic display. They showed that yaw motion in a direction consistent with visual circularvection enhanced that illusion, while contradictory motion cues caused a sudden loss of the visual illusion.

For the coordinated turn simulation under discussion, the most logical display strategy is a stripe roll velocity profile that is proportional to the roll velocity profile of the actual turn (see figure 2.4). This may enhance the roll velocity sensation produced by onset of Link roll thereby bringing roll rate perception closer to that of figure 2.14 (for $\tau_L = 5$). The work cited above [9, 10, 35] suggests the possibility that attitude perception will also be affected; however the true attitude profile can always be appropriately

adjusted. The work cited in reference 33 shows that yaw
circularvection builds gradually over 5 to 10 seconds.
Reference 13 cites an onset time of 3 to 4 seconds and a
peak response after 8 to 12 seconds for yaw CV. Roll into
the idealized turn of section 2.1 takes 3 seconds. If any-
thing, typical roll-in profiles are shorter than this. The
experiments described in Chapter IV of this thesis will
indicate that slow circularvection onset times pose a far
more serious consideration for the turn simulation than does
tilt illusion.

CHAPTER III

EXPERIMENTAL EQUIPMENT

3.1 Link GAT-1 Trainer

The Link GAT-1 Trainer has a one seat cockpit whose interior resembles that of a small, single engine, aircraft. Two translucent side windows subtend horizontal and vertical visual angles of about 50°. When gaze is directed straight forward, the windows cover a portion of the peripheral field beginning at a horizontal angle of about 40° on both sides.

The cockpit is mounted on a three degree of freedom motion base allowing only angular movement. Gimbal order, from outermost to innermost gimbal, is yaw, roll, then pitch. The base of the pilot seat is roughly 1 foot above the gimbal system center of rotation placing the occupant's head about 3.5 feet above the rotation axes. Gimbal angles are limited to 8° pitch down, 18° pitch up, and 12.5° roll to either side. There is no yaw angle limit but according to the user's manual the simulator is limited to yaw rates of up to 30° per sec. The absolute pitch and roll rate capability of the motion base is not listed in the user's manual, but maximum velocity attained during this work was 10° per second. A picture of the trainer appears in figure 3.1.

a. Exterior

b. Exterior showing
    stripe display

c. Interior showing handgrip
   device and meter

d. Interior showing
    handgrip device
    and pointer

Figure 3.1.   Modified Link Trainer

The Link is modified to be operated under the control of a hybrid computer. Inputs from the computer are sent through slip rings at the base of the Link and connected to the three drive motor amplifiers. The logic cards that normally command the amplifiers have been removed. Feedbacks are picked off from roll, pitch and yaw axis tachometers. These feedbacks are sent through the slip rings to the computer.

Figure 3.2 shows the control loops implemented by the analog computer. Note that the roll and pitch circuits are set up as position servos while the yaw circuit is a velocity servo. The actual analog board layout and trunk line arrangements are diagrammed in Appendix B. Figures 3.3 and 3.4 show pitch and roll frequency response of the Link when the set up shown in Figure 3.2 is used.

The roll and pitch systems are calibrated to $\pm$ 0.5° and the yaw system is accurate to $\pm$ 0.5°/sec. Scaling factors can be seen from Figure 3.2.

The Link trainer is outfitted with a projector and mirror apparatus capable of projecting stripes on the translucent side windows of the cockpit. The optics were originally designed by Robert Murphy (19) and the current system was built and installed by William Morrison. For this work, the system was configured to project horizontal stripes which move vertically, and in opposite directions on each window, as the film travels through the projector. Film speed is controlled with a variable speed servo-motor. The motor is

FIGURE 3.2   Servo loops and scaling implemented on the analog computer
for roll, pitch, yaw rate and stripe rate.

MAGNITUDE RATIO

Figure 3.3 Link roll and pitch magnitude ratio.

Figure 3.4 Link roll and pitch phase angle.

driven, through the slip rings, by a hardwired velocity servo loop and power supply in the Link room. Command signals to the velocity servo come through a trunk line from the computer. The optics are diagrammed schematically in Figure 3.5.

As viewed by a subject in the Link, each dark stripe subtends an angle of 12 degrees. The light space between them cover the same visual angle. It is not clear that subjects actually resolve the stripe image display at the distance of the window, and since the windows are nearly flat, distance from eye to stripe varies as a stripe moves up or down the window. For calibration purposes, roll velocity of the optokinetic display $(\dot{p}_{OK})$ was taken as a stripe speed along the window divided by half the width of the cockpit at eye level. The eye level width of the cockpit is about 30.5 inches (± 1/4"). The scaling used is shown in Figure 3.2.

The subject and the experimenter can communicate using a pair of headsets (one in the cockpit and one in the computer room). Since this audio system also picks up noise from the Link motion drive, a switch enables the subject to disconnect his earphones. The subject mike, however, remains active and the subject can always be heard by the experimenter.

In addition to the optical and audio systems, the trainer cockpit is equipped with a headrest, a black curtain covering the windshield and instrument panel, a green signal light, and a hand grip indicator device that is described in the next section.

left side mirror

beam
splitters

prism

front
window
covered

projector
with
continuous
film strip

(rotates
image 90°)

roof mirror   right side mirror

Figure 3.5 Stripe Projector Optics

3.2   Hand Grip Indicator Device

A hand grip device designed by Ahmed Salih [37]
has been modified to form the three degree of freedom
device diagrammed in Figure 3.6 and 3.7. It is essen-
tially a pistol grip handle mounted within a set of
gimbals. Gimbal order from outermost to innermost is
roll, pitch, then yaw. The roll gimbal is a Delrin
block bearing containing an aluminum shaft. Pitch
and yaw gimbal operation is obvious from the diagram.
Pitch and roll gimbal axes are connected to potentio-
meter shafts. The potentiometers are $5\Omega K$, single
turn, conductive plastic units guaranteed to $\pm$ 1%
independent linearity (Bournes model 3438).

Plus and minus 10 volts is sent from the analog
computer, through the Link sliprings, and placed across
the two potentiometers. The armature signals are run
back to the analog where they are buffered with an
analog amp (100 KΩ input impedance), and scaled to
yield a reading of gimbal angles.

The potentiometer load ratio is 20:1, and should
lead to no more than 0.75% load distortion. After
scaling errors are accounted for, gimbal angle readout
can be considered accurate to at least $\pm$ 5%. The roll

YAW
POTENTIOMETER
(NOT USED)

PISTOL GRIP

GIMBAL AXES INTERSECTION

DELRIN BEARING

ALUMINUM SHAFT

ROLL POTENTIOMETER

7.7"

5.0"

0.2"

ALUMINUM PLATE

0.5"

8.5"

9.2"

12.7"

Figure 3.6 Side view of handgrip indicator device.

Figure 3.7 Top view of handgrip indicator device.

armature signal can also be fed to a zero centered volt-
meter in the cockpit producing a needle deflection pro-
portional to hand grip roll angle. The face of the
meter is diagrammed in figure 3.8. The yaw axis was
not used for the work described in this thesis. Figure
3.9 shows the electrical set-up and scaling for the
hand grip and voltmeter system.

The hand grip device is installed in the Link
with its roll axis parallel to $\vec{i}_{xv}$ and its center of
rotation as shown in Figure 3.10. It can also be ad-
justed up to one inch forward (along $\vec{i}_{xv}$) from the
position depicted in Figure 3.10. The voltmeter is
installed so that it faces the subject and is located
thirteen inches above and three and one half inches
forward of the hand grip rotation center shown in
Figure 3.10. A thirteen inch pointer can be mounted
directly above the pistol grip so that it remains
parallel to the hand grip yaw axis. Figure 3.11
shows the pointer in place. Note that the orienta-
tion of the pointer with respect to the trainer cock-
pit is completely defined by the roll and pitch gimbal
angles of the hand grip device.

Figure 3.8 Face of zero centered meter used for roll rate
magnitude estimation task.

ANALOG COMPUTER   (Note: actual analog board layout is diagrammed in Appendix B)

Figure 3.9 Schematic of handgrip indicator and voltmeter setup.

Figure 3.10 Positioning of handgrip indicator.

CORK CAP

13.0"

POINTER

PISTOL GRIP

PITCH
POTENTIOMETER

Figure 3.11   Front view of handgrip device with pointer.

3.3   Hybrid Computer System

The digital element of the Man-Vehicle Laboratory hybrid system is a PDP-8 computer (4K words of core) equipped with two DEC tape drive units and a Model 33 teletype. The analog element is a GPS Model 290T 10 volt analog computer. The two communicate via 8 digital to analog channels, 7 analog to digital channels, and 12 control lines. Both machines have access to a digital clock. There are 40 analog trunk lines which have terminals on the analog board. These trunks can be connected directly to the peripheral equipment (strip chart, oscilloscope, FM tape recorder, etc.) and can also be connected to any of the 40 trunk lines extending from the computer room to the Link trainer experimental room.

Commands to the Link trainer are generated by the digital computer. Desired Link motion profiles are stored as a series of 20 line segment vertices. The computer connects the vertices by periodically

92

determining the value falling on a straight line
between the previous coordinate point and the next
coordinate point. These values are updated and
outputted on D/A channel 512 times per second.

The computer simultaneously generates four such
curves, all composed of twenty line segments. Each
curve is fed through a different D/A channel and
commands one of the four drive systems: Link roll
position; Link pitch position; Link yaw rate; and
projector film speed. At the beginning of a run, the
experimenter can select one of eight choices for each
of the four curves. A stimulus "package" contains
line segment vertices (pairs of magnitude and time
values) for up to 32 curves (4 curves times 8 choices)
and is stored in core.

In addition to outputting the four command signals,
the "operating program" starts the strip chart at the
beginning of each run (increases speed from 0.5 to 5 mm
per second), monitors feedback from the experiment, and
stops the strip chart when the run is over. The six
feedbacks monitored are the pitch and roll positions
of the Link trainer, the yaw velocity of the Link,
stripe display velocity, and pitch and roll gimbal angles

on the handgrip indicator. During some experiments, hand grip pitch feedback is replaced with Link roll tachometer feedback and roll gimbal angle feedback is scaled to represent the voltmeter needle deflection (see Figure 3.9).

The analog signals for the above quantities are fed to 6 A/D channels. The operating program samples these channels 5 times per second and stores the digitized samples sequentially in core. At the end of each run, the operating program dumps the data for that run onto magnetic tape. The first block (200_8 word locations) on each data tape is used as an index, the first location containing the number of the next available block and succeeding locations containing a list of previous "starting blocks". The second block is blank and is used as temporary storage. Every time a set of data is dumped onto tape, the operating program updates the tape index. When the computer is operating the Link, half core is reserved for output data, roughly one third is reserved for the stimulus input package, and the remaining sixth is occupied by the operating program.

A listing of the operating program appears in Appendix B. Also listed in Appendix B are programs used to initialize data tape indices and to access the data once on tape. Date reduction programs are discussed in Chapter V.

In addition to the digital data recording syztem, a four channel strip chart is used to continuously record four of the feedback quantities during experiment sessions. During

some of the experiments, a random noise input to the Link

roll drive is required. A pre-recorded random signal is

used for this and is piped from an FM tape recorder to the

analog computer where it is buffered, scaled, and added to

the roll position command. Figure 3.12 is a schematic

diagram of the entire experiment configuration.

Figure 3.12. Experiment Configuration.

CHAPTER IV

EXPERIMENTAL PROCEDURE

4.1   Experiment 1:   Roll Rate Calibration

Experiment 1 was designed to obtain subjective magnitude estimates of angular roll velocity during a standard type of stimulus in the Link trainer. The standard stimulus was a series of constant velocity rolls with a four second pause between each one. There was no yaw or pitch motion during this experiment, but there were three different types of visual stimulation. The projected horizontal stripes were either stationary on the cockpit side windows, rolled (moved up one side and down on the other) at a constant rate, or rolled at a rate proportional to the roll velocity of the Link trainer. The latter was achieved by using the roll tachometer feedback as a command signal to the film drive. There are two possible choices for the sign of the proportional stripe motion. Stripe motion can be opposite that of the Link (counterrolling stripes) or can be the same as the Link. Both strategies were used in this experiment. Counterrolling stripes with a gain of 1 implies that the stripes are stationary in inertial space, and provides a visual cue that is

completely consistent with actual motion. Counterrolling stripes will hereafter be referred to as having positive gains, since they provide a cue that complements Link motion. Proportional stripes rolling in the same direction as the trainer, and therefore providing a motion cue that contradicts the Link motion will be referred to as having negative gains. In the case of the constant stripe velocity stimulus, the stripe cue can be both complementary and contradictory during a single run depending on the direction of Link roll. For the proportional stripe motion, gains of 1, 2, 4, -1, and -4 were used. Constantly rotating stripes were run at 10°/sec, 20°/sec and 40°/sec.

Each run during an experimental session was 64 seconds long, the time required to fill up the section of the computer core reserved for feedback data. Four different roll sequences were used and were spaced more or less evenly throughout the session so that subjects could not easily become familiar with the profiles. The four profiles are shown in Figure 4.1. Each sequence contains roll rate commands of one, two, three, five, seven and ten degrees per second. The roll excursion angle varies with the stipulation that each motion must last at least 1.4 seconds. It was therefore difficult for subjects to use stimulus duration time as a criterion for their response.

In order to mask the vibrations characteristic of Link motion onset, a pseudo random noise signal was added to Link roll commands during every run. The noise signal was pre-

Figure 4.1 Position commands for calibration profiles.

recorded using a program written by Van Houtte [30], and is the sum of 20 sinusoids. The frequencies and magnitudes of the sinusoids are shown in Figure 4.2. The pattern repeats itself every 128 seconds and was scaled to produce a maximum velocity deviation of ± 1°/second. The roll position and velocity feedbacks produced by the noise signal alone are shown in Figure 4.3.

The voltmeter display connected to the hand grip roll axis (jumper plug in place and switch on in Figure 3.9) was used for subject indications. A 5°/sec roll, between + 7° and - 7° was used as a modulus, and corresponds to a 5 indication on the meter. A sequence of four such stimuli (two in each direction) was presented twice at the beginning of an experimental session and once before each run. The modulus sequence is shown in Figure 4.4. The following instructions were given to each subject:

"Use the head rest as a support or aid to keep your head stationary with respect to the cockpit. Keep your gaze on the meter. The meter needle can be moved by rolling the hand grip and will maintain a position proportional to the hand grip roll angle. When the experiment begins, concentrate on your sensation of roll rate or velocity. You will be given a motion called the modulus and your maximum sensation of roll rate during this motion should correspond to 5 on the meter. Subsequent motions

100

FREQUENCY	AMPLITUDE	PHASE (°)
F = 0.0151	A = 4.1259	Ø = − 88.33
F = 0.0227	A = 4.1259	Ø = + 92.98
F = 0.0380	A = 4.1259	Ø = − 85.86
F = 0.0532	A = 4.1210	Ø = + 96.06
F = 0.0837	A = 4.1406	Ø = + 99.58
F = 0.1296	A = 4.1210	Ø = − 75.41
F = 0.1752	A = 4.1162	Ø = − 70.13
F = 0.2211	A = 4.1259	Ø = +115.04
F = 0.2822	A = 0.4101	Ø = − 57.65
F = 0.3583	A = 0.4199	Ø = +130.69
F = 0.4499	A = 0.4101	Ø = − 38.23
F = 0.5568	A = 0.4199	Ø = +154.59
F = 0.6789	A = 0.4052	Ø = − 13.88
F = 0.8161	A = 0.4199	Ø = −177.36
F = 0.9687	A = 0.4150	Ø = −160.04
F = 1.1367	A = 0.4052	Ø = + 39.63
F = 1.3198	A = 0.4150	Ø = + 59.50
F = 1.5180	A = 0.4199	Ø = −100.01
F = 1.7470	A = 0.4101	Ø = +109.51
F = 1.9912	A = 0.4101	Ø = − 45.52

Amplitude Scale: 4.1259 = 1 volt

Figure 4.2 Frequency and phase spectrum of random noise signal.

Figure 4.3 Roll position and velocity feedback from Link trainer in response to random noise input.

Figure 4.4 Position command for modulus sequence.

should be rated proportionately; for example, a
roll rate that feels twice as fast as the modulus
should be 10 on the meter. The modulus will be
administered 8 times initially and then 4 times
before every run. During each run attempt to
continuously track your roll rate with the meter
needle. The first two runs will be practice. You
will be asked to switch off your earphones at the
start of each run. The experimenter will still be
able to hear you, so if your hand slips or you
make an involuntary indication for some other
reason, simply report the mistake verbally. The
green signal light will indicate that the run is
over and you may stop tracking and turn on your
headset. Remember to concentrate on your innate
feeling of roll velocity and do not attempt to
outguess the experiment. Indicate any roll rate
sensation you feel even if you can logically deduce
that the feeling is illusory."

The sequence or arrangement of runs for each session
was chosen to meet the following criteria:

1.   Since the stationary stripe category represents
        the standard to which other responses will be
        compared, it should be administered at least
        once using each of the four calibration profiles
        (Figure 4.1).

2.   To minimize order affects, no profile should ever be used twice in a row and they must be more or less evenly distributed throughout the session.

3.   The four stripe motion categories (stationary stripes, constant velocity stripes, proportional stripe motion with positive gain, proportional stripe motion with negative gain) must be distributed more or less evenly throughout the session and none should ever appear twice in a row.

4.   The different stripe gains and rates should appear in pseudorandom order.

5.   The number of runs per session must be held to 12 if possible and to no more than 13. This represents a one hour session and subjects tend to become bored and drowsy.

6.   At least four different arrangements meeting the above criteria should be presented to different subjects.

Figure 4.5 shows the four different arrangements that were used.

Feedback from the Link roll and pitch position potentiometers, Link roll and yaw tachometers, stripe speed tachometer, and the hand grip roll position potentiometer (indicating

STRIPE MOVEMENT CATEGORY

①

①	1	2	3	4
CAL1	3	1a		11a
CAL2	7	4c	2b	
CAL3	10	8b	5a	
CAL4	12	1	9c	6b

LINK MOTION

STRIPE MOVEMENT CATEGORY

②

②	1	2	3	4
CAL1	3		10a	12b
CAL2	5	1c	7c	
CAL3	9	6a	2b	
CAL4	11	8b		4a

③

③	1	2	3	4
CAL1	9	3b	1c	
CAL2	6		12a	2b
CAL3	10	7a		5a
CAL4	4	11c	8b	

LINK MOTION

④

④	1	2	3	4
CAL1	3	8a	5b	
CAL2	9	1c		11a
CAL3	7		2a	4b
CAL4	12	6b	10c	

(numbers in boxes are run numbers)

STRIPE MOVEMENT CATEGORIES:

1. Stripes fixed with respect to cockpit (SS).
2. Stripes constantly rotating with respect to cockpit.

    a. 10 deg/sec (SC10)
    b. 20 deg/sec (SC20)
    c. 40 deg/sec (SC40)

3. Stripe speed inversely proportional to Link roll rate (complementary to motion cue)

    a. Gain = 1 (SP1)
    b. Gain = 2 (SP2)
    c. Gain = 4 (SP4)

4. Stripe speed proportional to Link roll rate (contradictory to motion cue)

    a. Gain = -1 (-SP1)
    b. Gain = -4 (-SP4)

Figure 4.5 Run Sequence Arrangements for Experiment 1.

meter needle position) were recorded on digital tape. All
outputs except pitch position and yaw rate were also recorded
on the four channel strip chart.

4.2   Experiment 2: Roll Rate Estimation During Turn

Simulation

Experiment 2 was an attempt to obtain roll rate magnitude
estimates during three possible coordinated turn profiles.
One profile is that developed in Section 2.4 and will be ref-
erred to as the Ormsby model simulation or SIM1.   Another
profile simply multiplies the SIM1 profile by a factor of 2
and will be abbreviated SIM2.   The third profile (SIM3) is
the proportional roll strategy that would be followed by the
Link if it were using its own analog logic cards to simulate
the aircraft motion history of Figure 2.4.   The SIM1 and SIM2
motion profiles were combined with stationary stripes (SS),
stripes following the aircraft profile of Figure 2.4 (SA1)
and SA1 times a factor of 4 (SA4). Link feedbacks during
the three motion profiles are shown in Figures 4.6, 4.7 and
4.8. The first two are shown with SA1 stripe motion.

Criteria for run sequence arrangements were the following:

1.   No single motion profile should ever appear in
       two consecutive runs, and each should be spaced
       more or less evenly throughout the session.

Figure 4.6   SIM 1 with SA 1 stripe motion

Figure 4.7   SIM 2 with SA 1 stripe motion

Figure 4.8   SIM 3

109

2.   Within the SIM1 and SIM2 categories, a single stripe strategy should never appear in consecutive runs.

3.   The number of runs per session must never exceed 13.

4.   At least 4 arrangements meeting these criteria should be presented to different subjects.

The run sequence arrangements that were used are shown in Figure 4.9. The layout is even more uneven than that of Experiment 1. The SIM1 profile was considered the case of primary interest and the strategy was to insure that a significant number of data points were obtained for this case. The number of SIM2 and SIM3 runs were reduced in order to remain under the 13 run limit. Two calibration profile runs were included during each session as a check to see if the Experiment 1 calibration was still valid. Figure 4.9 shows the two practice runs at the beginning of each session. The first was always a calibration profile. It was hoped that this would reinforce the response scaling established by the subject during Experiment 1. The modulus routine (Figure 4.2) was administered twice at the beginning of the session and once before every run as in Experiment 1. Instructions to the subjects and outputs monitored and recorded were also the same as those in the first experiment.

Stripe Motion

① LINK MOTION

	SS		SA1		SA4	
SIM1	1	7	3	13	5	9
SIM2	2$_{pr}$	10	6		12	
SIM3	2	8				
CAL1	1$_{pr}$					
CAL2	4					
CAL3	11					

Stripe Motion

②

	SS		SA1		SA4	
SIM1	2	13	11	7	4	9
SIM2	2$_{pr}$	5	3		12	
SIM3	1	8				
CAL1	1$_{pr}$					
CAL2	10					
CAL3	6					

③ LINK MOTION

	SS		SA1		SA4	
SIM1	8	1	5	12	3	10
SIM2	2$_{pr}$	13	9		6	
SIM3	2	7				
CAL1	1$_{pr}$					
CAL2	4					
CAL3	11					

④

	SS		SA1		SA4	
SIM1	11	4	2	9	6	13
SIM2	2$_{pr}$	12	8		3	
SIM3	7	1				
CAL1	1$_{pr}$					
CAL2	5					
CAL3	10					

numbers in boxes are run numbers
subscript "pr" indicates practice run

Figure 4.9   Run sequence arrangements for experiment 2

4.3   Experiment 3: Vertical Tracking Task

Experiment 3 was designed to obtain subjective estimates of spatial orientation during coordinated turn simulations and during standardized pitch and roll stimuli. The simulation profiles used were the same as those used in Experiment 2 except that only SS and SA4 stripe motion was used. The standardized pitch and roll stimuli were   CAL2 and CAL3 from Figure 4.1. A third of these calibration runs were administered on the roll axis alone, a third used only pitch, and a third presented profiles on the pitch and roll axes simultaneously.

The hand grip indicator was outfitted with its pointer (see Figure 3.11), the face of the meter was covered, and the subjects were given the following instructions:

"Use the head rest as a support or guide to keep your head stationary in the cockpit. Keep your gaze near the top of the pointer. During each run, keep the pointer aligned with what you perceive as vertical with respect to the room. You will be asked to switch off your earphones at the start of the each run. The experimenter will still be able to hear you, so if your hand slips or you make an involuntary indication for some other reason, simply report the mistake verbally. The green signal light will indicate that the run is over, and you may stop tracking and switch your

earphones on. Remember to concentrate on your per-

ception of vertical and continuously track this direc-

tion with the pointer. Do not try to outguess the

experiment, and indicate your feeling of vertical

even if you can logically deduce that it must be

incorrect."

Note that since the handgrip and Link gimbal order is the

same for roll and pitch, subjective "response error" is just

the sum of the two roll gimbal angles and the sum of the two

pitch gimbal angles.

It was deemed important to have a significant number of

data points in the SIM1 category, since this is the simula-

tion of primary interest, and in the calibration category,

since this represents a base or standard. Other criteria are:

1.   No motion profile should ever appear in two con-
     secutive runs and every calibration profile
     should be followed by one of the turn simulation
     runs.

2.   Within the SIM1 and SIM2 categories, a single
     stripe motion strategy should never appear in
     two consecutive runs.

3.   The number of runs per session must not exceed
     16 (since it was not necessary to precede each
     run with a modulus, 16 runs represents a one
     hour time limit, as opposed to 13 runs in exper-
     iments 1 and 2).

4.   At least four arrangements meeting these
        criteria should be presented to different
        subjects.

The four run sequence arrangements used in Experiment 3 are
shown in Figure 4.10. The jumper plug (see Figure 3.9) was
not used and the corresponding switch was in the down posi-
tion during this experiment. Feedback from the Link roll
and pitch position potentiometers, the yaw tachometers,
stripe speed tachometer, and the handgrip position potentio-
meters were recorded on data tape as described in Section 3.3.
The hand grip feedbacks were calibrated to indicate gimbal
angles (see Figure 3.9). Hand grip outputs and the two Link
position outputs were also recorded on the four channel strip
chart.

4.4   Subjects

    Four naive subjects (non-pilots) and one pilot went
through all three experiments. During Experiments 2 and 3,
the pilot knew that some of the profiles were intended as
simulations of the Figure 2.4 turn profile. The naive sub-
jects did not know what any of the motions represented. Two
of the four naive subjects had been through earlier versions
of Experiments 1 and 3 and therefore had some experience with
the rate estimation and vertical tracking tasks. One of these

① Stripe Motion

Link Motion	SS			SA4		
SIM1	8	12	1	15	6	10
SIM2	2$_{pr}$		14	3		
SIM3	4		9			

Link Roll Motion

Link Pitch Motion	None	CAL2	CAL3	CAL1
None		2	13	1$_{pr}$
CAL2	11		7	
CAL3	5	16		

② Stripe Motion

Link Motion	SS			SA4		
SIM1	9	6	1	3	15	12
SIM2	2$_{pr}$		14	7		
SIM3	11		4			

Link Roll Motion

Link Pitch Motion	None	CAL2	CAL3	CAL1
None		10	8	1$_{pr}$
CAL2	2		5	
CAL3	16	13		

③ Stripe Motion

Link Motion	SS			SA4		
SIM1	13	2	7	4	10	16
SIM2	2$_{pr}$		14	8		
SIM3	5		11			

Link Roll Motion

Link Pitch Motion	None	CAL2	CAL3	CAL1
None		15	1	1$_{pr}$
CAL2	6		3	
CAL3	9	12		

④ Stripe Motion

Link Motion	SS			SA4		
SIM1	8	4	15	1	12	6
SIM2	2$_{pr}$		5	13		
SIM3	3		10			

Link Roll Motion

Link Pitch Motion	None	CAL2	CAL3	CAL1
None		9	11	1$_{pr}$
CAL2	16		7	
CAL3	2	14		

(all calibration profiles run with stationary stripe)

numbers in boxes are run numbers
subscript "pr" indicates practice run

Figure 4.10   Run sequence arrangements for Experiment 3

subjects underwent the current version of Experiment 2 twice due to an equipment failure the first time. Several subjects, besides the five mentioned so far, have undergone either earlier versions of one of the experiments, or sessions that were plagued by various equipment failures.

Every run is uniquely identified by three numbers: a subject number, a session number, and a run number. Subject numbers subscripted with a 'p' designate a pilot and run numbers subscripted with a 'pr' designate practice runs. Twelve subjects in all participated, but data is tabulated mainly for the five who successfully completed all three current experiments described in Sections 4.1, 4.2 and 4.3. Data from the other subjects and from earlier versions of the experiment will be quoted only when it helps clarify points raised by Experiments 1, 2 and 3.

The five "complete" subjects are numbers 2, 4, 9, 11_p, and 12. Figure 4.11 shows the experiment corresponding to each session for all 12 subjects. A 'prime' indicates an earlier version of the experiment and a superscript* indicates an equipment failure or mistake in administering the experiment. All sujbects are between the ages of 25 and 35 and to their knowledge have no vestibular deficiencies.

Several references have been made to earlier experiments. This applies only to Experiments 1 and 3 and these versions differed from the descriptions in this chapter in one or more of the following ways:

Subject No.	Session 1	Session 2	Session 3	Session 4	Session 5
1	Exp. 3'				
2	Exp. 3'	Exp. 1'	Exp. 1	Exp. 2	Exp. 3
3	Exp. 1'				
4	Exp. 1'	Exp. 1	Exp. 2*	Exp. 2	Exp. 3
5	Exp. 1'*	Exp. 3'			
6	Exp. 3'				
7	Exp. 3'*	Exp. 1'			
8	Exp. 3'*				
9	Exp. 1	Exp. 2	Exp. 3		
10p	Exp. 1*				
11p	Exp. 1	Exp. 2	Exp. 3		
12	Exp. 1	Exp. 2	Exp. 3		

' - early version of experiment   * mistake or malfunction during experiment

Figure 4.11   Experimental Sessions

1. Only two calibration profiles were used in
    Experiment 1 and the simulator excursion was
    always 14 degrees (between + 7° and - 7°).

2. No random noise or a much larger random noise
    was used in Experiment 1.

3. Different motion profiles and stripe motion
    strategies were presented in blocks instead of
    being distributed throughout a session.

4. More than 13 runs were used in Experiment 1 or
    more than 16 in Experiment 3.

5. Instead of the proportional stripe motion
    strategy in Experiment 1, stripes were moved at
    the same constant rate during each period of
    simulator roll motion.

4.5   Pilot Rating of Simulations

Two pilots were asked to rate seven turn simulations on
the basis of "realism". The pilots were presented with seven
different simulations consisting of combinations used and
order of presentation as shown in Figure 4.12. The pilots
were given a drawing of Figure 2.4 as well as a verbal des-
cription of this turn. It was suggested that they imagine
themselves copilots or passengers in a small aircraft, during
zero visibility conditions. The drawing, although studied

119

Subject	Run	Link Motion Profile	Stripe Motion Profile
10p	1	SIM2	SS
	2	SIM1	SA1
	3	SIM3	SS
	4	SIM2	SA4
	5	SIM1	SS
	6	SIM2	SA1
	7	SIM1	SA4
11p	1	SIM1	SS
	2	SIM3	SS
	3	SIM2	SA4
	4	SIM1	SA1
	5	SIM1	SA4
	6	SIM2	SA1
	7	SIM2	SS

Figure 4.12 Simulation profiles and order of presentation for pilot fidelity rating

before hand, was not taken into the cockpit.

The series of seven runs was presented twice. The first time, the subject was instructed to simply concentrate on his sensations as compared to those he would expect in a real aircraft. During the second presentation, which followed the same order as the first, the subject was told to mark his rating for each run on the form shown in Figure 4.13.

Each line of the form has 10 bins representing increasing "realism" from left to right. An indication at the far left means "not at all realistic" while an indication at the far right means "extremely realistic". Subjects were told to x the appropriate bin after each run using a new line each time.

The two subjects who participated in this were subjects 10_p and 11_p. Subject 10_p has a single engine, commercial instrument rating and 500 hours experience. Subject 11_p has a multiengine rating and over 1000 hours as an airforce instructor.

121

Realism

not at all   highly
realistic   realistic

1 ├──┼──┼──┼──┼──┼──┼──┼──┼──┼──┤

2 ├──┼──┼──┼──┼──┼──┼──┼──┼──┼──┤

3 ├──┼──┼──┼──┼──┼──┼──┼──┼──┼──┤

4 ├──┼──┼──┼──┼──┼──┼──┼──┼──┼──┤

5 ├──┼──┼──┼──┼──┼──┼──┼──┼──┼──┤

6 ├──┼──┼──┼──┼──┼──┼──┼──┼──┼──┤

7 ├──┼──┼──┼──┼──┼──┼──┼──┼──┼──┤

8 ├──┼──┼──┼──┼──┼──┼──┼──┼──┼──┤

9 ├──┼──┼──┼──┼──┼──┼──┼──┼──┼──┤

Figure 4.13   Simulation rating form

CHAPTER V

TABULATION OF DATA AND STATISTICAL ANALYSIS

5.1   Experiment 1: Roll Rate Calibration

Experiment 1 required subjects to track their roll rate
sensation during a series of constant velocity rolls (see
Figure 4.1) plus a low level random noise. Between runs sub-
jects were given several 5°/sec roll stimuli (the modulus)
and were told that this corresponded to a 5 on the response
scale. During the runs, subjects were instructed to use a
meter needle (controlled by a moving hand grip device) to
continuously indicate their sensations proportional to the
modulus. The stripe display was stationary during some runs
(SS), moved at different constant velocities during other
runs (SC), and moved with roll rates proportional to the Link
roll rate (SP) during some runs.

Figure 5.1 shows a typical continuous strip chart record-
ing of a run from Experiment 1. Figure 5.2 shows the same
run when played back from the digital tape record. Program
PLYBK, used to access the digital tape in this way is listed
in Appendix B. The first step in data reduction was to find
the peak roll rate stimulus and peak response indication for
each stimulus period. A stimulus period was taken as the time

Link
Roll
(deg.)

Subjective
Roll Rate
(response
scale)

Link
Roll Rate
(°/sec)

Stripe
Roll Rate
(°/sec)

1. 10

0

r. 10

r. 10

0

1. 10

1. 20

0

r. 20

1. 40

0

r. 40

|———————|
5 sec

Figure 5.1 Typical Strip Chart Recording of Roll Rate Magnitude Estimation During
Experiment 1. The motion profile is CAL2 (see figure 4.1), and the stripe
display remained stationary with respect to the cockpit (SS) during this run.
Subject 2, session 3, run 6.

Figure 5.2   The same Run Shown in Figure 5.1 Played Back From Digital Tape Using Program
            PLYBK.

from the onset of a link roll movement command to the onset
of the next movement command.

Stimulus and response peaks were computed directly from
the data tape by another PDP-8 program, ANAL1A, also listed
in Appendix B. In order to eliminate unwanted spikes, the
computer algorithm defines a peak as the maximum value remain-
ing equal to or less than the signal for longer than 0.2 sec-
onds. The computer identifies peak absolute values during
each stimulus period but outputs the value with their proper
signs. Stimulus peaks are computed from the Link tachometer
signal, and response peaks from the hand grip roll potentio-
meter signal. The former is scaled to deg/sec and the latter
to subject meter divisions (see Figure 3.8).

Figure 5.3 shows a typical printout from ANAL1A. "SET
PKG" referes to a separately compiled package that specifies
stimulus periods for each motion profile used. Each row under
the "INPUT" heading is the information that must be toggled
to the computer for each run to be analysed. "STARTING BLOCK"
refers to the location of the run on data tape; "SET NO"
refers to the motion profile used in that run (CAL1, 2, 3, or
4); and the next two numbers represent the data buffer posi-
tions of the stimulus and response signals. Buffer positions
for all the feedback signals recorded are listed in Appendix
B.

The output list is printed in order of decreasing stim-
ulus value. The signs actually refer to direction, with
plus (+) indicating right and minus (-) indicating left.

SUBJECT: 2-3   ③

DATE: 2/20/76

DATA TAPE: 3

SET PKG.: SPKG1

STIM. TYPE: S S

31 DATA PTS.;   4 SETS;   4 RUNS

INPUT: / BUFF. POSITION:

STARTING BLOCK	SET NO./	STIM.	RESP.
0456	01	06	05
0401	02	06	05
0514	03	06	05
0343	04	06	05

OUTPUT:

STIM. PK.	RESP. PK.
+ 9.20	+ 7.89
+ 8.63	+ 7.62
+ 8.34	+ 6.95
+ 6.28	+ 4.95
+ 6.21	+ 5.02
+ 4.49	+ 5.03
+ 3.95	+ 4.78
+ 3.92	+ 5.25
+ 3.10	+ 3.55
+ 2.36	+ 3.54
+ 1.88	+ 2.45
+ 1.37	+ 1.96
+ 1.28	+ 4.08
+ 1.10	+ 2.18
+ 1.05	+ 1.40
- 0.98	+ 0.19
- 1.35	- 1.47
- 2.01	- 2.13
- 2.14	- 1.69
- 2.23	- 2.14
- 2.35	- 1.97
- 2.81	- 2.44
- 2.95	- 5.07
- 3.03	- 1.96
- 3.36	- 2.88
- 4.16	- 2.74
- 4.80	- 5.69
- 4.86	- 5.37
- 6.00	- 6.48
- 6.12	- 5.09
- 8.82	- 5.73

Figure 5.3   Typical Printout From Program ANAL1A.   Output
quantities are peak roll velocity in °/sec
(STIM. PK.) and peak subjective roll rate estimate
in meter divisions (RESP. PK) achieved during each
stimulus period.   The 31 data points are from all 4
stationary stripe runs during the experiment 1
session.   Subject 2, session 3.

"STIM PK" units are deg/sec and "RESP PK" units are meter divisions.

If each stimulus response pair is considered a data point, each subject contributed 31 data points in the stationary stripe category, 7-8 data points for each of the gains used in the proportional stripe motion category, and 7-8 data points for each value of constant stripe motion. The latter case must be broken down further since during a given run, some Link motions were in the same direction as stripe motion and some were in the opposite direction. Thus within each constant stripe motion category 3-4 data points represent contradictory motion cues. The specific numbers vary slightly because two of the motion profiles have uneven numbers of left and right rolls (see Figure 4.1).

Data points were deleted only when the subject verbally indicated a slip of the hand or some similar error during the stimulus. There were only two such data points in all of Experiment 1.

In the stationary stripe category, there was a very strong correlation between stimulus and response points for all subjects. Correlation coefficients range from 0.96 to 0.98. Transformation of one or both variables with a log operator results in lower correlation, and linear regressions in all cases are significant at $\alpha = 0.001$. Figure 5.4 shows scatter plots for the cases of highest and lowest correlation. Figure 5.5 shows plots of residuals versus stimulus with

Figure 5.4 a.   Scatter Plot of Stationary Stripe, Calibration
Run Data Points For Subject 9. The abscissa is
the peak Link roll rate and the ordinate is the
peak subjective roll rate estimate during a
given stimulus period. Correlation coefficient
is .98, the highest recorded.

Figure 5.4 b.   Scatter Plot of Stationary Stripe, Calibration
                Run Data Points For Subject 4.   Correlation
                coefficient is .96, the lowest recorded.

Figure 5.5 a. Plots of STIM versus Residuals for stationary
stripe calibration regressions.

Figure 5.5 b. Plots of STIM versus Residuals for stationary
stripe calibration regressions. STIM is peak
Link roll rate, the independent regression
variable.

response as the dependent regression variable. The plots do show an increased variance at extreme values of the stimulus, but this is to be expected since a greater excursion is required of the response indicator when the stimulus is large, creating a more difficult manipulation task. In two cases (subjects 2 and 9) residuals show a tendency to be slightly above the abscissa for small positive stimuli and below for small negative stimuli. The effect, however, appears minor.

When response is taken as the dependent variable, the model is

$$RESP = B_0 + B_1 \text{ (STIM)} \tag{5.1}$$

The estimate computed from the data is

$$\hat{RESP} = b_0 + b_1 \text{ (STIM)} \tag{5.2}$$

where RESP is peak subjective angular rate indication during a stimulus period, and STIM is peak Link roll rate during the same period.

At a criterion level $\alpha = 0.01$, b_1 is not significantly different from 1.0 for any of the subjects nor is b_0 significantly different from zero. At the less stringent level of $\alpha = 0.1$, subject 4 shows a significant intercept and subjects 2 and 11 show slopes significantly different from 1.0. The statistic used to test the coefficient b_1 is

$$t_0 = \frac{b_1 - 1}{[\hat{V}(b_0)]^{1/2}} \tag{5.3}$$

and the test statistic for the intercept is

$$t_0 = \frac{b_0}{[\hat{V}(b_0)]^{1/2}} \qquad (5.4)$$

The mean value (± standard deviation) for b_1 across subjects is 0.96 ± 0.056. For b_0, the mean value is 0.21 ± 0.23. Mean variance of the estimate is 1.39 ± 0.44. Individual parameters for each subject are listed in Table 5.1.

A similar regression analysis was performed on the proportional stripe motion (SP) runs. During SP runs, stripes move at rates proportional to Link roll rate with proportionality constants 1, 2, 4, -1, and -4 (abbreviated SP1, SP2, SP4, -SP1, and -SP4 respectively). The sign of the gains refers to the direction of the visual motion cue with respect to Link motion. Positive gains indicate stripes providing a motion cue of the same direction as Link motion, while negative gains cause cues opposite to true roll direction. SP1 implies stripes that remain stationary in inertial space.

Figure 5.6 shows a typical SP run. Out of a total of 30 such runs, only 5 show regression slopes that differ significantly from the SS case for that subject at the $\alpha = 0.05$ level. Of those 5, three cases (subjects 9, -SP4; subject 12, -SP4; and subject 11_p, +SP4) have greater slopes and two (subject 2, SP4; subject 11_p, SP2) have smaller slopes than the SS case. Furthermore, there is no discernable pattern relating slope to proportional stripe gain. This is demonstrated in Figure 5.7.

Subject	Dependent (y) Variable	Regression Coefficient (b_1)	90% Confidence b_1	Intercept (b_0)	90% Confidence b_0	Variance of the Estimate	90% Confidence of Y given X
2	RESP	.909	± .074	.299	± .340	1.232	± 1.886
	STIM	1.032	± .084	-.298	± .363	1.399	± 2.010
4	RESP	1.044	± .094	.543	± .450	2.121	± 2.480
	STIM	.888	± .080	-.482	± .420	1.806	± 2.280
9	RESP	.943	± .062	.195	± .303	.989	± 1.690
	STIM	1.016	± .067	-.203	± .315	1.066	± 1.755
12	RESP	.991	± .070	-.082	± .327	1.146	± 1.819
	STIM	.962	± .068	.085	± .322	1.113	± 1.792
11p	RESP	.919	± .079	.109	± .372	1.484	± 2.070
	STIM	1.012	± .087	-.129	± .390	1.633	± 2.171

Table 5.1 Regression parameters for stationary stripe calibration runs. STIM is peak Link roll rate and RESP is peak, subjective roll rate estimation during a given stimulus period.

Figure 5.6 Typical Strip Chart Recording of Roll Rate Magnitude Estimation With SP4
Stripe Motion. The stripe roll rate is proportional to Link roll rate, but
4 times as fast and in a counter rolling direction. Subject 9, session 1,
run 9.

Figure 5.7   Slope, Intercept, and Variance for proportional (SP) and stationary (SS) stripe regressions. Independent regression variable is peak Link roll rate, and dependent regression variable is peak, subjective roll rate estimate.

Since stimuli of both signs (directions) are involved, any relation between intercept and proportional stripe gain would indicate some sort of visual, directional bias. Figure 5.7 shows no obvious intercept-gain relation. Figure 5.7 also contains a plot of "variance of the estimate" for each regression line against proportional stripe gain. Once again there is no clear relation with stripe gain although 6 of the individual points differ significantly from the SS case at the α = 0.05 level. These points are: subject 4, SP1 and -SP1; subject 9, SP4; subject 11_p, SP1; and subject 12, -SP4.

The above comparisons between proportional and stationary stripe cases contain the underlying assumption that SP cases, as well as the SS case, can be modelled by equation 5.1. As mentioned earlier, some residual plots show a slight tendency for responses to have greater magnitude than the regression estimates over low stimulus magnitudes. The same tendency sometimes appears in SP runs, and is, perhaps, more pronounced. An attempt was made to test for this without having to propose a specific model for SP. The appropriate technique is to test for differences in mean responses over the different conditions at a particular value of the stimulus. Because of the random noise input, there is never more than one sample at any precise stimulus value, so a small stimulus interval or bin must be used instead. An interval of 1°/sec was chosen as the smallest value that can be filled

with enough samples and the largest value that is still well
below the resolution of the response data (standard error of
the estimate was typically just over 1.0 on the SS regres-
sions). Even so, the only way to obtain enough samples is
to rectify the data and then either pool different SP gains
within subjects or pool all the subjects. In order to min-
imize subject and sign (direction) affects, response data
points for each subject were transformed by the SS case,
stimulus dependent regression. When stimulus is taken as
the dependent variable, the regression is a least squares
estimate of the stimulus, given some response value. By
employing this estimate, each response, for all stripe motion
cases, can be transformed into the stimulus value most likely
to have produced that response had stripes been stationary.
The effect is to remove any directional bias or non-unity
gain characteristic of a particular subject. In other words,
the stationary stripe regressions were used as calibration
curves. Figure 5.8 shows a plot of stimulus versus trans-
formed response (RESP') for subject 9 during SP1, SP2, and
SP4 runs. Note that the SS regression line is represented
by a line of unity slope passing through the origin (the
solid line in the figure). The dotted lines form a 90% confi-
dence interval taken from the original SS curve. The parti-
cular stimulus bin chosen was the interval from 2 to 3°/sec.
This interval contains the largest sample density across the
population and is near the middle of the region where the

Figure 5.8   STIM versus RESP' for SP1, SP2, and SP4 data points, subject 9.
RESP' is peak, subjective, roll rate estimate transformed by the
stationary stripe calibration regressions.   The stationary stripe
regression line is represented by STIM = RESP'.

phenomenon in question is observed. The test statistic is

$$t_0 = \frac{(\overline{RESP'}_{SP} - \overline{RESP'}_{SS})}{s_p(\frac{1}{n_{SP}} + \frac{1}{n_{SS}})^{1/2}} \qquad (5.5)$$

where s_p is the pooled variance, n is sample size and $\overline{RESP'}$
is the mean transformed rectified response. The null hypo-
thesis is

$$H_0: \quad \overline{RESP'}_{SP} = \overline{RESP'}_{SS}$$

The test was tried in two ways. Each subject was tested indi-
vidually by pooling SP1, SP2 and SP3. Each of the preceeding
stripe motion categories (SP1, SP2, and SP3) was tested indi-
vidually by pooling all subjects. Use of pooled variance
implies that the true variances of the underlying distribu-
tions are equal. A test for difference in variance is
insignificant for all cases at the $\alpha = 0.1$ level.

Only subject 11_p showed a significant difference, at the
$\alpha = 0.1$ level, between SS and SP stripe motion. When subjects
are pooled, $\overline{RESP'}_{SP4}$ is greater than $\overline{RESP'}_{SS}$ at a significance
level $\alpha = 0.025$. SP1 and SP2 categories show longer mean res-
ponses than SS although not significantly so, even at the
$\alpha = 0.1$ level. The means and standard deviations for all
cases are shown in Table 5.2.

Evaluation of the constant stripe motion (SC) data was
seriously hampered by the small number of available data
points in each category. Figure 5.9 shows a typical SC run.

SUBJECT	$\overline{RESP'}_{SS}$	$\overline{RESP'}_{SP}$
2	3.01 ± 1.18	2.53 ± 0.78
4	2.64 ± 0.93	3.06 ± 1.16
9	3.06 ± 0.99	3.28 ± 0.96
12	2.31 ± 1.25	1.99 ± 0.58
11_p	2.51 ± 1.08	3.31 ± 1.06

Table 5.2 RESP' during stationary stripe runs ($RESP'_{SS}$) and

RESP' during proportional stripe runs ($RESP'_{SP}$) for

stimuli between 2 deg/sec and 3 deg/sec. The pro-

portional stripe column is composed of pooled samples

from all 3 positive gains (visual cue in the same

direction as true motion). RESP' is the mean of

roll rate estimate responses that have been trans-

formed by calibration regressions and rectified

(given positive signs).

Figure 5.9   Typical Strip Chart Recording of Roll Rate Magnitude Estimation During SC20
Stripe Motion.   Stripe display rolls at 20°/sec to the right throughout the
run.   Subject 9 session 1, run 8.

Regression lines, in many instances have no statistical sig-
nificance, and those that do pass a statistical test must
still be viewed with the understanding that they depend on
only 4 data points. The constant stripe motion was always
to the right with respect to the Link cockpit, so Link rolls
to the left (negative stimulus values) provide complementary
vestibular and visual cues, while rolls to the right (posi-
tive stimulus values) presented contradictory vestibular cues.
The word "complementary" is used to indicate that visual
motion cues are in the same direction as actual Link motion.
"Contradictory" implies the opposite. Positive and negative
(right and left) stimulus values were therefore worked up as
separate regressions. Intercept, slope, and variance of the
estimate values are presented in Figure 5.10 only for those
regressions showing statistical significance. (Numbers fol-
lowing the "SC" abbreviation refer to the constant stripe
velocity in degrees per second.)

The figure does show a tendency towards lower (more
negative) intercept values during "complementary" constant
stripe motion and during 40°/sec "contradictory" constant
stripe motion than in the SS case. The magnitudes involved
are on the order of 1°/sec which is rather small. Slopes
tend to be smaller in all 3 complementary SC categories than
SS. Slopes are smaller than SS in the contradictory 10°/sec
and 20°/sec stripe categories, but tend to be larger in the
contradictory 40°/sec case. For SC10 and SC20, differences

Figure 5.10 Slope, intercept and variance for constant velocity (SC) and
stationary stripe (SS) regressions. Peak response is the
dependent variable. "Complementary" refers to data points
during left Link rolls, consistent in direction with the
visual cue. "Contradictory" referes to right roll data points,
contradicted by the visual cue.

from SS can be explained by the small nonlinear trend dis-
cussed earler in terms of residual plots. It can be ex-
pected to show up in the SC regressions since each includes
stimulus values on only one side of the origin. The SC40
data, on the other hand, may show a real response bias
caused by the stripes, especially at low stimulus values.
In order to check this without the linearity assumptions
implied by the regression analysis, the SC data was trans-
formed and tested under the same procedure used for the SP
data. The only difference was that individual subjects
could not be tested. Only by pooling subjects are enough
data points available. The results show larger $\overline{RESP}'_{SC}$ than
$\overline{RESP}'_{SS}$ but differences are not significant either for indi-
vidual stripe speeds or when all speeds are pooled.

5.2   Experiment 2: Roll Rate Estimation During Turn

Simulation

During Experiment 2, subjects performed the same roll
rate estimation task as in Experiment 1, but the stimulus
profiles included three variations of a coordinated turn
simulation in combination with three different moving stripe
profiles. One simulation profile is the profile found to
produce nearly the same model estimate of attitude perception
as the idealized aircraft turn, and is abbreviated SIM1. SIM2

has a roll profile proportional to SIM1 but twice the mag-
nitude, and the profile abbreviated SIM3 employs a roll
profile proportional to aircraft roll (proportionality con-
stant = 1/6). The profiles are shown in Figures 4.6, 4.7
and 4.8. The three stripe display conditions are stationary
stripes (SS), and stripe roll rates proportional to true
aircraft roll rate (SA). In the latter case, proportionality
constants of 1 (SA1) and 4 (SA4) were used. Two calibration
runs (CAL) with stripes stationary were also administered
during the course of each Experiment 2 session.

Figures 5.11 and 5.12 show two typical responses to SIM1.
Note that in the former, the subject has responded to all the
stimuli while in the latter there is a response only to the
two rolls away from zero (the first and third roll motions).
Figures 5.13 and 5.14 show responses to SIM2 and SIM3 respec-
tively. The simulation profile data was reduced using a
PDP-8 program that is a slightly modified version of ANAL1A
and is compiled as ANAL1B. The only difference is that the
output list is printed in the order of input and is not
ordered by stimulus size. A different set package (SPKG2) is
also used and stimulus periods are defined as shown in Figure
5.15. The stimulus periods will be referred to as STIM #1,
STIM #2, etc. A typical output from ANAL1B is shown in Figure
5.16. This printout gives the peak roll rate stimulus and
peak response for several runs of SIM1, therefore the "SET NO"
is 1. Each block of four output data points corresponds to

Figure 5.11 Strip Chart Recording of Roll Rate Magnitude Estimation During SIM1 Turn Simulation Profile. SIM1 is the profile found to produce nearly the same model estimate of attitude perception as the idealized aircraft turn. Subject 4, session 4, run 8.

Figure 5.12 Strip Chart Recording of Roll Rate Magnitude Estimation During SIM1.
Comparison of Link roll rate (channel 3) and subjective response (channel 2)
shows no response to the second and fourth stimuli. Subject 2, session 4,
run 11.

Figure 5.13   Strip Chart Recording of Roll Rate Magnitude Estimation During SIM2 Turn
Simulation Profile.   Roll magnitudes are twice those of SIM1.   Subject 9,
session 2, run 10.

Figure 5.14 Strip Chart Recording of Roll Rate Magnitude Estimation During SIM3. SIM3 is the proportional roll simulation strategy applied to the idealized turn of section 2.1. Subject 4, session 4, run 2.

151

Figure 5.15 Set Package SPKG2, used to analyze roll rate magnitude estimation data
during turn profiles. The diagram shows stimulus periods below corres-
ponding motion profiles. "Stimulus period" is the interval over which
the stimulus and response peaks are evaluated.

SUBJECT: 9 -2   (1)

DATE: 3/9/76

DATA TAPE: 3

SET PKG.: SPKG2

STIM. TYPE: SIM 1

24 DATA PTS.;   2 SETS;   6 RUNS

INPUT: /   BUFF. POSITION:

STARTING BLOCK	SET NO./	STIM.	RESP.	
1055	01	06	05	SS
1207	01	06	05_	
1113	01	06	05	SAI
1341	01	06	05	
1151	01	06	05	SA4
1245	01	06	05_	

OUTPUT:

STIM. PK.	RESP. PK.	
- 1.76	- 2.02	
+ 1.45	+ 1.17	
+ 1.53	+ 1.11	
- 1.72	+ 0.05	SS
+ 1.60	+ 2.51	
- 1.76	+ 1.54	
- 1.73	- 3.76	
+ 1.40	- 2.16	
- 1.77	- 1.45	
+ 1.44	- 0.40	
+ 1.70	+ 3.46	
- 1.77	+ 3.43	SA1
+ 1.62	+ 1.58	
- 1.68	+ 1.93	
- 1.85	- 1.71	
+ 1.56	+ 1.66	
- 1.86	- 1.92	
+ 1.38	- 2.14	
+ 1.56	+ 2.66	
- 1.67	+ 3.51	SA 4
+ 1.66	+ 2.91	
- 1.70	+ 2.92	
- 1.78	- 2.23	
+ 1.53	- 1.74	

Figure 5.16   Typical Printout From Program ANAL1B.   Output
quantities are peak Link roll rate (°/sec) and
peak, subjective, roll rate estimate (meter
divisions).   The motion profile is SIM1, so there
are 4 data points per run (see figure 5.15) and
these are bracketed.   Corresponding stripe
profiles are also indicated.

153

STIM #1 through STIM #4 from a single run. The runs are in order of input. All three stripe motion strategies appear on the same printout and runs have been marked by hand with corresponding stripe motion codes. Analysis is based on 6 runs of SIM1 per subject (2 runs per stripe profile times 3 different profiles), 3 runs of SIM2 (1 run of each stripe profile) and 2 runs of SIM3 (both with SS stripe).

The missed responses observed in Figure 5.12 are of interest because they were not anticipated. For tabulation purposes, a missed response was defined to be a response to STIM #2 or #4 (STIM #1 and #3 were never "missed") either less than 10% of that subject's average STIM #1 and #3 response magnitude or of a sign opposite to the stimulus. The latter condition usually indicates that the response from STIM #1 did not quite return to zero by the time STIM #2 began. The total miss ratio (number of misses divided by number of possible responses) over all subjects and stripe profiles is just over 2/3. Individual results are listed in Table 5.3. Note that if a subject were responding to the visual cue as opposed to vestibular or tactile cues, the Figure 5.12 response profile would be expected during SA1 and SA4 runs.

A contingency table was set up for SIM #2 and #4 responses with two columns, "responded" and "missed"; and three rows, SS, SA1 and SA4. Data for the table was pooled from all subjects. A χ^2 test indicates that the null hypothesis of

MOTION PROFILE	STRIPE PROFILE	SUBJECT	2	4	9	11_p	12	M_r/n_r
SIM1	SS	M/n	3/4	2/4	3/4	1/4	2/4	11/20 = 0.55
	SA1	M/n	4/4	3/4	3/4	2/2	2/4	14/18 = 0.78
	SA4	M/n	4/4	1/4	4/4	2/4	4/4	15/20 = 0.75
		M_c/n_c	11/12	6/12	10/12	5/10	8/12	40/58 = 0.69
SIM2	SS	M/n	1/2	0/2	0/2	0/2	0/2	1/10 = 0.10
	SA1	M/n	1/2	0/2	2/2	0/2	0/2	3/10 = 0.30
	SA4	M/n	2/2	0/2	2/2	1/2	1/2	6/10 = 0.60
		M_c/n_c	4/6	0/6	4/6	1/6	1/6	10/30 = 0.33

$n \equiv$ number of samples

$M \equiv$ number of misses

$n_r \equiv$ row total; $n_c \equiv$ column total

$M_r \equiv$ row total; $M_c \equiv$ column total

Table 5.3 Miss ratio during roll rate estimation task. Miss ratio is the number of times a subject failed to respond to a stimulus divided by the number of such stimuli. Only the second and fourth stimuli of turn simulation profiles SIM1 and SIM2 (see Figure 5.15) are considered.

155

independence between columns and rows cannot be rejected. Therefore, although a slightly higher miss rate was recorded during the moving stripe runs, the optokinetic stimulus had no statistically significant effect on the phenomenon.

During SIM2 runs, misses of STIM #2 and #4 were not as frequent, but still occurred. The total miss rate is 1/3 as opposed to 2/3 for SIM1. Individual results are shown in Table 5.3. Notice that there are only half as many data points as for SIM1. A χ^2 contingency test is significant at the $\alpha = 0.1$ level, but not if a more stringent criterion is used. SA stripe profiles may contribute to missed responses during SIM2 runs; however, the low significance of the results coupled with the small number of data points and the lack of significance for the same tests in the SIM1 case, suggests that a cautious interpretation is appropriate.

STIM #1 and #3 response magnitudes show no statistical relation to the stripe motion profile for either SIM1 or SIM2. During SIM1 runs, these responses did tend to be slightly larger than predicted on the basis of SS calibration runs (discussed in Section 5.1). The affect is significant at $\alpha = 0.05$ for subjects 2, 4, and 9. The two calibration runs during Experiment 2 sessions are not significantly different from those obtained during Experiment 1 for any of the subjects. As discussed several times, residuals for subject 2 and 9 calibration regressions are slightly biased in the stimulus direction for low stimulus values. The average mag-

nitude of this effect is 0.58 for subject 2 and 0.26 for subject 9. If appropriate corrections are made, significance of the above effect is lost for subject 2. During SIM2 runs, only subjects 4 and 11 responded with significantly greater than expected magnitudes to STIM #1 and #3. Individual means for SIM1, SIM2 and SIM3 are listed in Table 5.4. During SIM3, subjects 2, 4, and 12 were not significantly different from their respective calibration regression lines, but subjects 9 and 11_p responded with a significantly greater magnitude. SIM3 means are based on 4 data points per subjects (2 runs times 2 roll motions per run).

5.3   Experiment 3

Experiment 3 employed both the calibration (CAL) and turn simulation (SIM1, SIM2, and SIM3) profiles, but the subjective task was to continuously estimate earth vertical, not roll velocity as in Experiments 1 and 2. Subjects attempted to align a pointer, mounted on the hand grip indicator with their estimate of earth vertical. The calibration profiles (see Figure 4.1) were used on the pitch axis alone and the roll axis alone as well as on both simultaneously (see Figure 4.10).

MOTION PROFILE	SUBJECT	RESPONSE TO STIM #1 & #3†	RESPONSE TO STIM #2*& #4*†	MEAN STIMULUS VALUE (deg/sec)
SIM1	2 4 9 11 12 P	2.31 ± 0.63 2.31 ± 0.35 2.28 ± 0.81 1.89 ± 0.91 1.61 ± 0.57	----** 1.30 ± 0.48 1.42 ± 0.35 1.36 ± 0.72 1.00 ± 0.40	1.64 ± 0.12
SIM2	2 4 9 11 12 P	3.13 ± 0.52 5.13 ± 0.62 3.66 ± 0.11 4.41 ± 0.49 3.00 ± 0.74	1.38 ± 0.53 2.06 ± 0.53 2.84 ± 0.90 3.32 ± 1.27 1.65 ± 0.45	3.38 ± 0.21
		POOLED RESPONSES TO STIM #1 AND STIM #2		
SIM3	2 4 9 11 12 P	2.18 ± 0.59 1.88 ± 0.32 3.19 ± 1.05 3.42 ± 1.06 1.74 ± 0.41		1.61 ± 0.04

* only values scored as "responses" are included.
**no response to STIM #2 or STIM #4
† mean ± standard deviation

Table 5.4 Mean, roll rate estimate response magnitudes (RESP), and roll rate stimulus magnitudes (STIM) during turn simulations. (For clarification of "STIM #" see Figure 5.15)

Figure 5.17 is a typical strip chart recording made during a CAL profile run in Experiment 3. Note the quantities output on the chart are slightly different from those shown in Experiments 1 and 2. The first channel still carries Link roll position, but channel two is now scaled to indicate hand grip roll angle instead of meter divisions. Channels three and four contain Link and hand grip pitch position, while the Link roll and film strip tachometer signals are no longer displayed at all. The Experiment 3 CAL runs were reduced with a digital program called ANAL2, a printout of which appears in Figure 5.18. The input quantities are the same as those in ANAL1A. Output quantities are defined as follows. "DS" is the peak change in stimulus from its initial value over a stimulus period ("initial" refers to the start of the stimulus period). Note that the stimulus for Experiment 3 is either Link roll position or Link pitch position and the program deals with only one of these at a time. The print-out shown in Figure 5.18 is concerned with pitch position as indicated by the entry in the input table under "BUFF POSITION" (buffer position 1 is the Link roll potentiometer signal, position 2 is the pitch potentiometer signal, and 5 and 6 correspond to the hand grip and pitch potentiometers respectively). Peaks are defined by the same algorithm used in ANAL1A and 1B. "DR" is the same function as DS, but applied to the response (hand-grip roll or pitch angle). "ADR-ADS" is an error computation

4-5-16

Link
Roll
(deg.)

1. 10

0

r. 10

Subjective
Roll
(deg.)

1. 10

0

r. 10

Link
Pitch
(deg.)

up 10

0

dwn. 10

Subjective
Pitch
(deg.)

up 10

0

dwn. 10

5 sec

Figure 5.17   Typical Strip Chart Record of Two Axis Vertical Tracking Task With
Calibration Profiles on Both Roll and Pitch Axes.   The roll Profile is
CAL2 and the pitch profile is CAL3 (see figure 4.1).   Subject 4, session 5,
run 16.

SUBJECT: 2 - 5

DATE: 3/24

DATA TAPE: 3

SET PKG.: SPKG 3

STIM. TYPE: CAL (pitch)

32 DATA PTS.;   4 SETS;   4 RUNS

INPUT: / BUFF. POSITION:

STARTING BLOCK	SET NO./	STIM.	RESP.	
1567	02	02	06	no roll
2111	03	02	06	no roll
1644	02	02	06	CAL3 on roll axis
2034	03	02	06	CAL2 on roll axis

OUTPUT:

	DS		DR		ADR-ADS		SVEL	SDUR	RLAG	RDUR	SET	STIM
-	4.83	-	1.66	-	3.17	-	0.96	5.00	3.60	8.60	2	1
+	11.86	+	9.38	-	2.47	+	2.96	4.00	2.20	6.20	2	2
-	13.72	-	11.38	-	2.33	-	9.81	1.40	2.00	5.00	2	3
+	9.52	+	7.08	-	2.44	+	1.98	4.80	3.60	8.40	2	4
-	9.17	-	7.82	-	1.35	-	5.10	1.80	1.60	5.60	2	5
+	11.86	+	9.38	-	2.47	+	6.57	1.80	2.20	4.60	2	6
-	7.32	-	8.97	+	1.64	-	3.05	2.40	1.40	6.00	2	7
+	2.39	+	2.84	+	0.45	-	0.98	2.40	2.80	4.20	2	8
-	6.93	-	4.57	-	2.35	-	2.05	3.40	2.20	6.60	3	1
+	13.81	+	15.34	+	1.52	+	9.87	1.40	1.60	2.20	3	2
-	10.98	-	11.32	+	0.34	-	5.00	2.20	1.80	5.40	3	3
+	8.83	+	7.75	-	1.08	+	2.94	3.00	2.00	6.20	3	4
-	11.86	-	9.46	-	2.40	-	6.59	1.80	2.00	4.60	3	5
+	5.90	+	1.85	-	4.05	+	2.95	2.00	6.00	4.80	3	6
+	7.91	+	6.45	-	1.45	+	4.94	1.60	3.60	4.80	3	7
-	6.93	-	1.94	-	4.99	-	0.98	7.00	6.80	9.80	3	8
-	4.83	-	4.45	-	0.37	-	0.96	5.00	1.60	7.20	2	1
+	11.86	+	5.60	-	6.26	+	2.96	4.00	2.60	4.40	2	2
-	13.67	-	9.54	-	4.12	-	9.77	1.40	2.20	2.00	2	3
+	9.42	+	3.52	-	5.89	+	1.96	4.80	4.20	8.40	2	4
-	9.47	-	6.37	-	3.10	-	5.26	1.80	3.80	5.40	2	5
+	11.86	+	12.13	+	0.26	+	6.57	1.60	2.20	5.40	2	6
-	7.56	-	5.06	-	2.50	-	3.14	2.40	3.60	6.00	2	7
+	2.44	+	0.52	-	1.91	+	1.01	2.40	6.40	6.00	2	8
-	6.98	-	4.85	-	2.12	-	2.06	3.40	2.60	6.20	3	1
+	13.91	+	9.27	-	4.63	+	9.93	1.40	5.40	5.00	3	2
-	10.93	-	8.03	-	2.90	-	4.98	2.20	2.00	5.80	3	3
+	8.88	+	6.04	-	2.84	+	2.96	3.00	2.60	6.60	3	4
-	11.66	-	8.44	-	3.22	-	6.48	1.80	2.40	5.60	3	5
+	5.85	+	4.00	-	1.85	+	2.92	2.00	3.20	4.80	3	6
+	8.05	+	4.08	-	3.96	+	5.02	1.60	5.60	5.20	3	7
-	7.03	-	5.15	-	1.87	-	1.01	7.00	0.80	4.00	3	8

Figure 5.18   Typical Printout From Program ANAL2   For Calibration Runs.   Data channels being analysed are Link pitch angle and subjective pitch angle.

which will also be referred to as "E" and is defined

$$E = (DR - DS)(\text{sign of DS}) \tag{5.6}$$

A positive E always indicates a response of greater magnitude
than the stimulus in the direction of the stimulus. A nega-
tive E indicates a response that is smaller than the stimulus
or in the wrong direction. Stated in still another way, if
E's are positive, the subject is overestimating the stimulus,
and if they are negative, he is underestimating or going the
wrong way. "SVEL" is the average velocity of the stimulus
and "SDUR" is the duration of the stimulus. Both these quan-
tities are computed over the time of commanded roll or pitch
motion, not the entire stimulus period (see Section 5.1 for
the definition of "stimulus period"). "RLAG" is the time
from the start of the stimulus period until the response
reaches the magnitude of SVEL. This value was almost always
reached by the response during the calibration runs. Since
an x°/sec stimulus will reach x° in 1 second, RLAG is 1 when
the response follows the stimulus exactly. An indication of
the amount by which the response lags behind the stimulus is
RLAG - 1 seconds, and will be referred to as the "lag factor".
"RDUR" is the time for the response to reach DR. Both RLAG
and RDUR have maximum values equal to the stimulus period
duration. SET and STIM # have already been defined, the for-
mer corresponding to a set of stimulus periods (in this case,
one of the 4 possibilities from SPKG1, the same package used

in Experiment 1) and the latter specifying a stimulus period within that set.

Table 5.5 lists some parameters computed from ANAL2. There are several interesting things to note. Although different subjects respond with quite different gains, as can be seen from the mean response magnitude and mean errors, correlation between DR and DS is always quite high within each category. This indicates that subjects are self consistent and respond in a fairly linear fashion over the stimulus range. Differences in parameters are usually larger and are more often significant between pitch and roll categories than between single axis and two axis motions within subjects.

Having to track both a roll and a pitch motion simultaneously does not seem to hamper accuracy significantly during this experiment although it does cause slightly slower responses. RLAG is an average of 0.29 seconds longer when there is motion in both the pitch and roll axes, but across subjects, the data shows no significant difference between the mean of RMS percent error values in single and two axis motion categories.

There does not seem to be any trend among subjects regarding differences between pitch and roll response. Some subjects show a more accurate response to roll stimuli while others show a more accurate pitch response (lower RMS percent error). This is a little bit surprising considering that

SUBJ	MOTION AXIS	$\|\overline{DS}\|$ (°)	$\|\overline{DR}\|$ (°)	E (°)	σ_E (°)	RMS % ERROR	% ERROR	σ %ERROR	$\overline{RLAG}$ (SEC)	σ_{RLAG} (SEC)	$\overline{SDUR}$ (SEC)	$\overline{RDUR}$ (SEC)	$\rho_{DS,DR}$	$\rho_{RLAG,SVEL}$
2	R	8.9	4.8	-4.15	1.70	54	49	22	3.91	2.26	2.88	5.35	0.97	+0.30
	R+	8.8	4.3	-4.50	1.70	55	53	16	4.50	1.38	2.88	5.80	0.97	+0.35
	P	9.0	7.3	-1.66	1.89	35	28	21	2.84	1.57	2.88	5.81	0.97	-0.48
	P+	9.0	6.1	-2.96	1.76	39	35	19	3.20	1.55	2.88	5.52	0.98	+0.12
4	R	8.9	14.5	+5.90	5.96	85	68	51	1.64	0.96	2.88	5.38	0.95	-0.46
	R+	8.9	12.7	+3.80	4.71	59	47	37	2.08	1.80	2.88	5.41	0.97	-0.58
	P	9.0	11.5	+2.50	2.38	42	34	26	1.70	1.30	2.88	5.58	0.99	-0.32
	P+	9.0	11.4	+2.40	3.14	47	39	27	2.16	1.32	2.88	5.48	0.98	-0.04
9	R	8.9	7.5	-1.35	2.36	39	30	26	2.80	1.57	2.88	5.11	0.96	-0.63
	R+	8.9	8.5	-0.80	3.87	56	41	40	2.89	2.45	2.88	4.94	0.92	-0.41
	P	9.0	12.3	+3.22	4.62	70	51	49	2.53	1.19	2.88	5.31	0.95	-0.30
	P+	9.0	10.6	+1.34	4.00	60	44	41	2.41	1.62	2.88	5.15	0.95	-0.20
11_p	R	8.9	11.2	+2.20	3.32	46	37	28	2.20	1.71	2.88	4.93	0.97	-0.59
	R+	8.9	11.4	+2.50	5.40	73	52	52	2.53	1.83	2.88	5.03	0.60	-0.57
	P	9.0	11.6	+2.60	2.70	38	29	24	2.03	1.00	2.88	5.43	0.98	-0.57
	P+	9.0	13.6	+4.50	3.59	65	56	34	2.25	1.29	2.88	5.44	0.98	-0.50
12_p	R	8.9	12.3	+3.45	4.69	57	43	39	1.63	1.38	2.88	3.95	0.96	-0.34
	R+	8.9	12.6	+3.19	7.14	92	73	57	2.23	1.78	2.88	5.00	0.84	-0.30
	P	9.0	20.4	+11.36	5.85	144	128	67	1.64	1.15	2.88	4.33	0.97	-0.52
	P+	9.0	15.9	+6.83	3.90	93	81	48	1.56	0.71	2.88	4.88	0.97	-0.04

R ≡ Roll axis data, no pitch motion; P ≡ Pitch axis data, no roll motion; R+ ≡ Roll axis data, simultaneous pitch motion; P+ ≡ Pitch axis data, simultaneous roll motion; σ_x ≡ standard deviation of x; $\rho_{x,y}$ ≡ coefficient of correlation between x and y.

Table 5.5 Means, standard deviations, and correlations computed from ANAL2 parameters. The data is from vertical tracking task, calibration profiles.

subjects must rely to some extent on depth perception to gauge the pitch position of the hand grip pointer (see Figs. 3.10 and 3.11). It was expected that pitch judgements would be consistently less accurate. Subjects 4, 11_p, and 12 all tend to overestimate and indicate larger pitch and roll deviations than the true stimuli (E is always positive); subject 2 tends to underestimate the change in roll and pitch angle; while subject 9 tends to overestimate pitch changes and underestimate roll changes. The difference between pitch and roll $\bar{E}$ are significant for all subjects except 11_p at an $\alpha = 0.05$ level. Across subjects, there is no significant difference between the mean of RMS percent error values in the pitch and roll categories.

RLAG (the time for change in response position to reach the magnitude of the stimulus velocity) shows little correlation to SVEL. The correlation coefficient tends to be negative, but is small and in most cases is not significantly different from zero.* This implies that within the accuracy of the data there is very little dependence of RLAG on the stimulus velocity although there might be some tendency towards slightly faster responses to larger stimulus velocities.

---

*For a sample of 16, the correlation coefficient must be greater than 0.5 to be significant at the 0.05 level [1,27].

Means ± standard deviations of some of the individual means and deviations listed in Table 5.5 are as follows:

$|\overline{DS}|$	8.95 ± 0.06	
$|\overline{DR}|$	11.03 ± 3.84	
$\overline{E}$	2.02 ± 3.83	
standard deviation of $\overline{E}$	3.73 ± 1.58	
RMS percent error	62.5 ± 25.9	
$\overline{RLAG}$	2.44 ± 0.77	
standard deviation of $\overline{RLAG}$	1.49 ± 0.42	
$\overline{SDUR}$	2.88 ±	
RDUR	5.19 ± 0.45	

ANAL2 was also used to reduce the simulation profile data from Experiment 2. A different set package, SPKG3, was used for these runs and Figure 5.19 shows the stimulus periods for each set. Figure 5.20 is a typical printout for a series of SIM1 runs. The stimulus and response axis being examined (in this case roll) is again indicated by the buffer position values, and the stripe profile corresponding to each run has been marked by hand. All input and output list quantities are the same as described earlier in this section.

Figures 5.21 and 5.22 show two strip chart recordings of a SIM1 run. Figure 5.21 is typical of most subjects in that first and third roll motions are clearly indicated, while second and fourth barely receive any indication at all. The phenomenon is essentially the same as that discussed in

Figure 5.19 Set Package SPKG3, Used to Analyze Vertical Tracking Task
During Turn Simulations. The diagram shows stimulus period below cor-
responding motion profiles. Stimulus period is the interval over which
stimulus and response peaks are evaluated.

SUBJECT: 12-3   (7)

DATE: 4/2

DATA TAPE: 5

SET PKG.: SPKG-3

STIM. TYPE: SIM1 (roll)

36 DATA PTS.;   3 SETS;   6 RUNS

INPUT: / BUFF. POSITION:

STARTING BLOCK	SET NO./	STIM.	RESP.	
1074	01	01	05	
1170	01	01	05	SS
1341	01	01	05	
1017	01	01	05	
1132	01	01	05	SA4
1264	01	01	05	

OUTPUT:

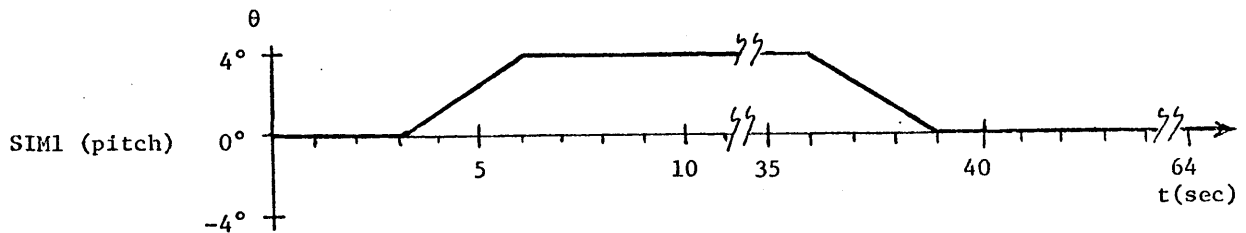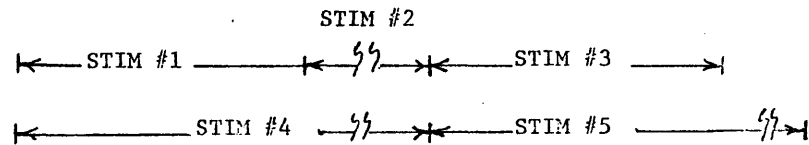| DS	DR	ADR-ADS	SVEL.	SDUR	RLAG	RDUR	SET	STIM
- 1.96	- 6.51	+ 4.55	- 1.96	1.00	1.40	4.80	1	1
+ 1.95	- 0.87	- 2.83	+ 1.95	1.00	5.00	4.00	1	2
+ 1.85	+ 4.72	+ 2.86	+ 1.85	1.00	2.40	4.20	1	3
- 1.91	+ 0.92	- 2.84	- 1.91	1.00	5.00	1.20	1	4
+ 1.96	- 2.45	- 4.41	+ 0.07	26.02	19.81	28.02	1	5
- 1.95	+ 3.03	- 4.99	- 0.09	20.62	24.62	24.02	1	6
+ 1.97	+ 11.56	+ 9.58	+ 1.97	1.00	1.00	4.60	1	1
- 1.94	+ 1.68	- 3.62	- 1.94	1.00	5.00	2.20	1	2
- 1.90	- 22.35	+ 20.44	- 1.90	1.00	1.40	2.40	1	3
+ 1.90	+ 6.78	+ 4.88	+ 1.90	1.00	3.60	2.60	1	4
- 1.97	+ 2.73	- 4.71	- 0.08	26.02	19.61	19.21	1	5
+ 1.90	+ 8.30	+ 6.39	+ 0.08	20.62	0.20	14.81	1	6
+ 1.97	+ 3.85	+ 1.87	+ 1.97	1.00	3.00	4.20	1	1
- 1.84	- 3.50	+ 1.66	- 1.84	1.00	2.20	2.40	1	2
- 1.96	- 8.19	+ 6.22	- 1.96	1.00	1.60	3.00	1	3
+ 1.84	+ 6.35	+ 4.51	+ 1.84	1.00	0.80	4.00	1	4
- 1.85	- 4.45	+ 2.60	- 0.07	26.02	2.00	15.61	1	5
+ 1.84	+ 11.35	+ 9.50	+ 0.08	20.62	0.60	23.82	1	6
- 1.96	- 5.24	+ 3.28	- 1.96	1.00	1.00	4.00	1	1
+ 1.96	+ 0.39	- 2.35	+ 1.96	1.00	5.00	3.40	1	2
+ 1.90	+ 5.15	+ 3.24	+ 1.90	1.00	1.60	4.40	1	3
- 1.80	+ 0.20	- 2.01	- 1.80	1.00	5.00	3.20	1	4
+ 1.96	+ 1.19	- 0.76	+ 0.07	26.02	8.40	18.01	1	5
- 1.83	+ 0.78	- 2.61	- 0.09	20.62	3.60	21.42	1	6
- 1.92	- 5.84	+ 3.91	- 1.92	1.00	0.80	3.80	1	1
+ 1.90	- 0.08	- 1.98	+ 1.90	1.00	5.00	3.80	1	2
+ 1.80	+ 7.28	+ 5.48	+ 1.80	1.00	2.00	4.80	1	3
- 1.86	+ 3.57	- 5.44	- 1.86	1.00	5.00	4.40	1	4
+ 1.90	+ 6.01	+ 4.11	+ 0.07	26.02	3.60	27.42	1	5
- 1.89	+ 4.15	- 6.04	- 0.09	20.62	0.20	18.01	1	6
+ 1.92	+ 0.31	- 1.61	+ 1.92	1.00	5.00	1.40	1	1
- 1.86	- 0.14	- 1.72	- 1.86	1.00	5.00	0.40	1	2
- 1.95	- 11.59	+ 9.64	- 1.95	1.00	1.40	4.20	1	3
+ 1.84	- 1.07	- 2.91	+ 1.84	1.00	5.00	1.20	1	4
- 1.86	- 1.69	- 0.17	- 0.07	26.02	0.40	28.82	1	5
+ 1.87	+ 9.89	+ 8.02	+ 0.08	20.62	5.00	24.22	1	6

Figure 5.20   Typical Printout From Program ANAL2 For Turn
Simulation Runs.   Data channels being analysed are
Link roll angle and subjective roll angle.

Figure 5.21 Strip Chart Record of Two Axis Vertical Tracking Task During SIM1 Turn
Simulation Profile. Notice that the subjective roll response does not
follow the shape of the Link roll profile. There seems to be no response
corresponding to the two rolls back to vertical. Subject 11_p, session 3,
run 8.

Link
Roll
(deg.)

1. 10

0

r. 10

Subjective
Roll
(deg.)

1. 10

0

r. 10

Link
Pitch
(deg.)

up 10

0

dwn. 10

Subjective
Pitch
(deg.)

up 10

0

dwn. 10

5 sec

Figure 5.22 Strip Chart Record of Two Axis Vertical Tracking Task During SIM1 Turn
Simulation Profile. This subject has vigorously responded to all 4 roll
motions although he has overestimated the roll angles. Subject 4, session
5, run 6.

Section 5.2 except that perception of roll attitude instead of roll rate is involved. Figure 5.22 shows a response characterized by vigorous indication of all stimuli and is typical only of subject 4. Figure 5.23 shows the group mean and individual means of E during STIM #1, #2, #3 and #4. No significant stripe profile effects were found for any of the variables in any of the subjects, so the different stripe profiles have been pooled yielding 6 samples per subject for each stimulus period. The differences between responses to the first and third and the second and fourth roll stimuli is quite apparent in the figure. Note that not only is subject 4 the exception by virtue of responding to all stimuli, but his responses are all much larger than those of most other subjects as though he has made himself especially sensitive to roll cues. Most subjects responded with a greater percent error than the range displayed during calibration runs, the exceptions being subjects 2 and 12. All subjects, except 2, overestimated their roll angles during STIM #1 and #3. The other point of interest in Figure 5.23 is the large variance among subjects both in mean response and standard deviation.

It should be pointed out that roll DS magnitude (change in Link roll angle during a given stimulus period) during SIM1 is always 2° (± 0.2°) which is smaller than any stimulus administered during CAL runs and also is of shorter duration than any CAL stimuli. SIM2 employs rolls (4° ± 0.3°) that

Figure 5.23   Mean, roll axis E value for each subject during the first four
stimulus periods of SIM1. (See Figure 5.19 for a diagram of the
stimulus periods).   DS ≡ change in stimulus angle and DR ≡ change
in response angle. A positive E indicates overestimation of roll
angle, a negative E represents underestimation, and an E value
below -2° (DR' = 0) is a response in the wrong direction.

are included in the range of the CAL run stimuli, although
duration of roll velocity is still only 1 second. Figure
5.24 shows E means during SIM2 and is based on 2 runs per
subject. Subjects still tend to show less response to STIM #2
and #4 than to #1 and #3, but the difference is significant
at the 0.05 level only for subject 11$_p$. Experiment 3 did not
include runs of SIM1 or SIM2 with yaw and pitch motion omitted,
but several such runs were obtained by accident during an
earlier version of Experiment 3. The two subjects involved
were subjects 7 and 8 (see Figure 4.11). During these sessions,
yaw was not functional and during a couple of runs, pitch was
accidently left off also. As seen in Figure 5.25, the same
asymmetrical response appears in one of the runs. This by no
means represents a significant demonstration, but is at least
a tentaive indication that roll responses might be similar to
those found in Experiment 3 even in the absence of yaw and
pitch motions.

STIM #5 and STIM #6 were included in set 1 (see Figure
5.19) in order to see if there was any significant tendency
for roll angle estimations to gradually return towards zero
between STIM #2 and #3 and after STIM #4. Figure 5.25 might
suggest that this is the case, however, mean responses over
STIM #5 and #6 indicate no significant trend.

Figure 5.26 plots E for pitch response to SIM1 and SIM2.
The pitch stimuli were always noticed. STIM #2, #4 and #5
responses are not displayed in Figure 5.26.   They were in-
cluded in set 2 (see Figure 5.19) for the same reasons STIM #5

Figure 5.24 Mean, roll axis E value for each subject during the first four
stimulus periods of SIM2.

Link
Roll
(deg.)

Subject 7

Subjective
Roll
(deg.)

l. 10⁻

0

r. 10⁻

l. 10⁻

0⁻

r. 10⁻

Link
Roll
(deg.)

Subject 8

Subjective
Roll
(deg.)

l. 10⁻

0

l. 10⁻

l. 10⁻

0

r. 10⁻

5 sec

Figure 5.25 Strip Chart Records Showing Link Roll Angle and Subjective Roll Angle During
Two Runs With No Pitch or Yaw Motion. Subjects 7 and 8.

Figure 5.26   Mean, pitch axis E values during SIM1 and SIM2.

Figure 5.27 Typical Strip Chart Record of Vertical Tracking Response to SIM3. SIM3 is the proportional roll strategy for simulating the idealized turn of section 2.1. Subject 4, session 5, run 4.

176

Figure 5.28 Mean roll axis E values during SIM3. Positive E indicates overestimation of roll angle, negative E represents under-estimation, and an E value below -5 deg (DR' = 0) is a response in the wrong direction

and #6 were included in set 1, and also showed no significant trends.

Figure 5.27 is a typical strip chart recording of a SIM3 run. All subjects show a definite response to both roll in and roll out motions, and indicate a sustained roll angle during the body of the turn. Figure 5.28 plots E for roll response to SIM3 and is based on 2 runs per subject.

5.4   Pilot Rating of Simulations

Seven different combinations of simulation motion profile and stripe display profile were presented to two pilots for evaluation as turn simulations (see Figure 4.12). Table 5.6 shows the ratings assigned each simulation profile by the two pilots. Markings on the rating forms (see Figure 4.13) were scored by assigning numbers 1 through 10 to the bins from left to right. A "10" indicates that the simulation felt very realistic, while a "1" indicates that it did not feel at all realistic. Both pilots preferred the SIM1 profile (the profile shown by the Ormsby model to closely match the attitude sensations in a real aircraft) over the other two choices. There is some conflict between the two pilots concerning the stripe profile preferred, and in fact neither pilot is very self consistent in this aspect. The ratings suggest that the motion profiles were more important to the pilots than the stripe cue, although one of the pilots

MOTION PROFILE	STRIPE PROFILE	PILOT RATING	
		SUBJECT 10$_p$	SUBJECT 11$_p$
SIM1	SS	6	8
	SA1	5	9
	SA4	6	8
SIM2	SS	3	7
	SA1	4	6
	SA4	2	8
SIM3	SS	3	3

Table 5.6   Pilot ratings of simulation profiles. "10" is the highest
"realism" rating (extremely realistic) and "1" is the
lowest (not at all realistic).

(11_p) did comment afterwards that he preferred the "slow stripes" (SA1).

SIM3, the proportional roll strategy, received a relatively low rating from both pilots. In this profile, a roll angle is maintained throughout the body of the turn (see Section 2.4 and Figure 4.8). 11_p commented that he felt a "side force" during this run, and 10_p said that the maneuver felt like a "slipping spiral". Comments from both pilots about SIM1 and SIM2 (SIM2 is proportional to SIM1, but with twice the roll angle magnitude) emphasized that the motions were too "jerky", "mechanical", "bumpy" or "abrupt". There are two factors besides the simulation strategy that probably contribute to this. Pitch and roll motion in our Link trainer is characterized by a certain bumpiness that is a combination of mechanical vibrations and position potentiometers that have a tendency to become dirty and a bit noisy. The coordinated turn profile being simulated is an unusually mechanical maneuver itself. Roll in and roll out of this idealized turn are far more abrupt than a turn initiated by a real pilot. It is not surprising for this to be reflected by the simulations.

CHAPTER VI

DISCUSSION OF RESULTS

6.1   General Observations on Roll Rate Magnitude

Estimation Task

During a series of constant velocity rolls between 1 and

10 degrees per second, between 2.5 and 14 degree excursion,

and in the presence of a superimposed low level noise ($\pm 1°/s$),

subjects are able to produce continuous magnitude estimates,

the peaks of which correlate very highly with stimulus velo-

cities. Input-output functions appear to be linear relations,

in most cases not significantly different from

$$RESP = B_1(STIM) \qquad\qquad (6.1)$$

By setting a 5 response equal to 5°/s as a modulus for this

experiment, B_1 was effectively set to 1. Accuracy of the

subjective data, defined by a 90% confidence interval, is

about $\pm 2°/s$.

The proportional relation of equation 6.1 is somewhat

surprising since psychological scaling laws are commonly log

functions or power laws [28]. The data may represent

a small segment of a much larger log or power curve, or may
be a reflection of the response scale and modulus employed.
Psychological estimates are very sensitive to the precise
layout of the response task [24]. The modulus was defined
midway along both the response scale and stimulus range, and
stimuli were distributed over a range that corresponded
closely to the range of numbers on the response scale (the
meter of Figure 3.8). If subjects simply tend to use the
entire, or almost the entire, response range available to
them, a linear function would be the result. Whatever the
reason, the proportional response function is very conveni-
ent and useful as a calibration device. It is important to
note that the modulus was repeated several times before
every run during the roll rate magnitude estimation experi-
ments.

There is evidence of a slight breakdown of the linear
response at low stimulus values for two subjects. It seems
reasonable to assume that the response magnitude will tend to
level off as stimulus threshold is approached, but this work
did not attempt to carefully investigate threshold phenomena.

6.2   General Observations on Two-Axis Vertical
                  Tracking

There is considerable variance among subjects in the
gain with which they estimate their orientation using the
continuous vertical tracking task described in Section 4.3

(subjects attempt to keep a pointer aligned with earth vertical). For excursions ranging from 2.5 to 14°, some subjects consistently overestimated their roll and pitch angles, in one case by as much as 100%, while others consistently underestimated these angles. Subjects are quite self-consistent however, and within subjects, changes in indicated orientation angle correlate highly with true attitude changes. Simultaneously tracking different profiles on the pitch and roll axes (as opposed to motion in only one axis) does not significantly affect performance during the relatively simple, low frequency stimuli used in Experiment 3. As seen in Figure 5.21, the response follows the shape of the stimulus profile rather faithfully. The lag factor discussed in Section 5.3 (time for the response to reach a value equal to the stimulus velocity minus the time for the stimulus to reach that value) ranged from roughly 1-2 seconds and is not significantly dependent on stimulus velocity. With system dynamics as predicted by the Ormsby model, the lag factor is several tenths of a second. This implies that there is a 1-2 second response lag inherent in the task. It must be assumed that most of this delay is not due to the perceptual mechanism but to transferal of perceptions to the appropriate response.

The overall implication is that the two dimensional tracking task is a very useful tool for obtaining attitude perception information so long as the frequency range of

interest is low. For instance, if the response task is modelled as a transport lag of 1 second plus a first order dynamic lag with a time constant of 0.55 seconds, the resulting lag factor is 1.5 seconds for a stimulus like the standardized rolls and pitches of Experiment 3 (see Figures 4.1 and 5.21). Other combinations of transport delay and dynamic lag would also be consistent with the data, but any reasonable combination leads to an effective bandwidth of under 0.25 Hz after which the subject could not be expected to track effectively. It would be useful to try the vertical tracking task over a range of higher frequencies than those used here to verify this.

6.3   Optokinetic Display and Visual Effects

The moving stripe display (described in Section 3.1) had little if any effect on either roll orientation or roll velocity estimates during the experiments described in Chapter IV, with two possible exceptions. When data from all subjects is pooled, roll rate magnitude estimates during 2 - 3° per second stimuli in Experiment 1 (roll rate magnitude estimation during standardized roll stimuli) show a mean that is 0.82° per second higher for SP4 stripe motion than for stationary stripes. SP4 means that the horizontal stripes "rolled" on the cockpit side windows at a rate four

times cockpit roll rate and in a direction opposite the cockpit, thus providing a visual cue consistent in direction with true cockpit motion. Although the effect is significant, it is very small and represents a bias that is below the standard deviation of the responses. Proportional stripe motion with smaller gains produced no such effect. It might be interesting to try the same thing using still higher stripe gains.

In the case of the simulation profiles, one of which employed roll velocities of the same magnitude involved in the above discussion, the stripes had no effect on response magnitude. They may, however, have contributed to the frequent failure of subjects to detect two of the stimuli during SIM2 (turn simulation with a roll profile proportional to that predicted as optimum by the Ormsby model, but twice the magnitude - see Figure 4.7). The result does make sense because during the two stimuli in question, the optokinetic cue contradicts cockpit roll direction; but the significance of the result is very low. The effect cannot be demonstrated at all for SIM1 (turn profile predicted as optimum by the Ormsby model - Figure 4.6) perhaps because the detection failure occurred so often even without the stripes. This will be discussed further in the next section. The lack of dramatic stripe effects on response magnitudes, while a bit disappointing, is not at all surprising. As mentioned in Section 2.5, there is literature showing that about the yaw

axis, circularvection takes at least 5 to 10 seconds to build [3, 33], and most roll stripe motion periods in the experiments of this thesis are of shorter duration. The exception is the constant stripe rate runs of Experiment 1, but in this case, the stripe cue was contradicted by the true motion much of the time. In the case of circular-vection about a vertical axis, there is evidence that a complementary yaw motion reduces circularvection onset time [33]. It was hoped that this would be the case for horizontal circularvection also, however roll and pitch rotations bring the otoliths as well as the canals into play, creating a somewhat different situation. Because of the otoliths, the vestibular system has a much stronger low frequency contribution to pitch and roll orientation perception than is the case for yaw. It is very difficult to completely disorient a person with respect to vertical in a normal 1 g environment.

An unintentional but unavoidable factor introduced by having an illuminated cockpit is the visual frame effect. Lichtenstein and Saucer [17] using the classic rod and frame test [31] have shown that some people have a very strong tendency to align their perceived vertical with any reference frame visible in their environment. Subjects were asked to align a rod with vertical. The rod was "framed" by a rect-angle that could be rotated by the experimenter. Some sub-

jects tended to align the rod with the frame up to about 10° deviation from vertical. There are a couple of basic differences between the experiment just quoted and the Link trainer experiment. Although there were ample reference lines available in the cockpit even with a curtain in front of the subject, the available frames are not quite as well defined or compelling as in the reference frame experiment. In the Link, th subject was rotated along with the visual cockpit reference, while in Lichtenstein and Saucer's experiment only the reference frame was moved.

If the frame effect were to manifest itself during the Link experiment, it would be expected to attenuate responses by encouraging subjects to keep the hand grip aligned with the cockpit vertical ($\vec{i}_{zv}$). Although one subject did consistently underestimate orientation angles, other subjects consistently overestimated them and there is no way to tell whether the frame effect played a part. It was definitely exhibited by one phenomenon that does not show up in the data tabulation. Often, during Experiment 3, when the experimenter flashed the signal light indicating the end of a run, a roll or pitch indication that had been sitting perhaps 3 or 4 degrees off vertical would suddenly snap back. Subjects realized that at the finish of a run the cockpit was probably level and they took the opportunity to realign their indication using the cockpit as a reference.

No extensive attempt was made to eliminate cockpit reference
frames. They are certainly present in the real aircraft and
simulator cockpits towards which the results of this work are
aimed, and it was felt that any such effects might as well
be included in the data.

The fact that roll vertical alignment responses do not
show any strong tendency to be more accurate than pitch res-
ponses across subjects is a little surprising since depth
perception is involved in the pitch task. One subject actu-
ally complained about the pitch task, saying he was very
unsure of the pointer's pitch alignment. Interestingly, his
data shows a greater accuracy in pitch than in roll response.
There are two possible interpretations of this result. One
is that depth perception of the hand grip is more accurate
than other elements of the task causing its effect to be
buried in the noise. The other possibility is that vision
is not terribly important to the performance of the task.
A series of runs in a completely dark cockpit would help to
clarify this.

6.4   Implications for the Ormsby Model

The high correlation between roll velocity estimation
and true stimulus value in Experiment 1 is supportive of the

model. The data is too noisy, however, to allow much comparison of the response dynamics with the model. Figure 6.1 shows the Ormsby model predictions of roll rate perception during a series of stimuli similar to the calibration profiles of Experiment 1. Roll rate perception peaks within a fraction of a second of stimulus onset and then begins to decay. When the stimulus returns to zero the rate perception undershoots by an amount equal to its previous decay. The entire decay and overshoot effect amounts to less than 1 degree. This is below the accuracy of the peak responses themselves in the data. The small dynamic effects predicted by the model are probably overshadowed by the dynamics of the conscious control task and the manual control dynamics involved in quickly moving the meter needle to its target position. It may be useful to look at the calibration profiles with a stochastic version of the Ormsby model (see Chapters 5 and 6 and [21]). Variances could be compared to the subjective data and if the model is assumed correct, it may be possible to separate the noise introduced by the response task from that inherent in the perceptions themselves.

The high stimulus-response correlation in the vertical tracking data is also supportive of the model. The variance

roll rate (°/sec)

Input to vestibular model

× × × × × Model estimate of roll rate perception

t (sec)

190

Figure 6.1   Model prediction of roll rate perception during stimulus similar to experiment calibration runs

across subjects is certainly noteworthy but the model cannot be expected to predict this. Ideally, the model should represent the population norm or mean. As mentioned in Section 6.2, responses usually follow the shape of the calibration profiles more or less faithfully (see Figure 5.21), but beyond this the model predicts no dynamic effects of a large enough magnitude to be seen through the noise of the data.

The only finding that is decidedly contrary to the Ormsby model predictions is the frequent failure to detect the two roll motions towards vertical during SIM1 and SIM2 (the simulation suggested as optimum by the Ormsby model and a proportional profile employing larger roll angles - see Figures 4.6 and 4.7). During SIM1 roll rate estimation responses, this failure was observed in over 2/3 of 58 possible responses (see Table 5.3). The effect is also apparent in the vertical tracking data as shown in Figures 5.27 and 5.28. Ormsby model predictions can be seen in Figures 2.16 and 2.17. There are several possible explanations. Perhaps a threshold effect is being observed. The computer model used in this thesis does not consider thresholds. The motions involved ($>2°$ tilt and $>2°/sec^2$ angular acceleration) are above generally accepted threshold values. Otolith threshold is often quoted as about 0.005 g $= 0.3°$ tilt [18, 21, 36] and the bulk of data on canal angular

acceleration threshold varies roughly between 0.1° and 1.5°
per second^2 [4, 5, 6, 20, 21], although there are some fig-
ures outside this range. These threshold values are usually
applied to deviation from zero, under optimum detection con-
ditions, and often employ longer duration accelerations than
are used here. If, for instance, the stochastic threshold
model discussed by Ormsby [21] is employed, it is conceivable
that the results observed during SIM1 will be predicted since
the dynamics of the first motion (away from vertical) will
effect threshold to the second (back to vertical). SIM2, on
the other hand, employs large enough roll angles (>4°) and
accelerations (>4°/sec^2) to make this seem unlikely as a
complete explanation.

Another possible explanation is a blocking effect in
which the second of a pair of motions is not being observed
due to the nature of the response task. Note that there is
only a two second interval between the first and second
motions of each pair (see Figures 4.6 and 4.7 roll profiles).
This is shorter than the four second intervals used between
stimuli during the calibration profiles and on the order of
the response lag discussed in Section 6.2. Remember that
even if the response task is modelled as a transport delay
and dynamic lag, this pathway involves a conscious evaluation
of sensations by the subject and transferral to an open loop
manual task. It is reasonable to assume that the period
from the onset of a stimulus until the subject has settled on

an indicator position requires increased concentration and attention on the part of the subject. If onset of each rolling motion is thought of as a detection problem it can be assumed that if a subject's attention is still focused on a response to the first stimulus of a pair, he has a higher probability of missing the second. Furthermore, it is also reasonable to assume that this probability will be inversely related to the stimulus magnitude. SIM2 then, having the same roll profile but with twice the magnitude of SIM1, would be expected to exhibit a lower incidence of detection failures.

Still another possibility is that there is some difference inherent in detecting a roll towards vertical as opposed to away from vertical. This sounds like a rather unlikely explanation since total deviations from vertical are so small (2° for SIM1 and 4° for SIM2).

The final possibility is that the Ormsby model dynamics should be revised to account for this result. It could be done by adding lag somewhere to make the system behave more like an integrator of the short duration roll stimuli in SIM1 and SIM2; however, this would contradict responses observed during the calibration profiles (see Figures 5.1 and 5.21) and during SIM3 (proportion roll strategy - see Figure 5.16 and 5.31). It would mean responses to these stimuli should be much more gradual than those observed. In fact if the response to SIM1 shown in Figure 5.25 is

compared to the SIM3 response shown in Figure 5.31, it will
be seen that they are nearly identical in time course. It
is very difficult to see how this could be explained by man-
ipulating the model dynamics. The most probable explanation
then,is a combination of the detection threshold inherent in
perception, perhaps modelled as Ormsby's stochastic threshold
model (see Chapters 5 and 6, [21]), and an added probability
of detection failure introduced by the response task itself.

During the roll angle tracking task, once subjects have
indicated correctly a roll away from vertical and have "missed"
the roll motion back to vertical, they can most often be ob-
served to maintain their incorrect roll angle indication until
the next stimulus occurs. Occasionally they will drift slowly
towards zero or make a sudden shift back towards zero after
from 5 to 30 seconds. There is evidence that once people
commit themselves to a decision they will stick with it until
it becomes obviously untenable [11]. If a subject begins to
feel that his roll angle indication is incorrect, but has
noticed no motion, it seems likely that he will exhibit a
tendency to stick by his indication as long as possible.

Two Ormsby model time constants were discussed at length
in Chapter II (Section 2.3) in relation to predicted sensa-
tions during aircraft coordinated turns. One constant, τ_E
(see Figure 2.9), is used to highpass filter unconfirmed
canal estimates for the DOWN estimator. The other, τ_L

(see Figure 2.10), is used to high pass filter canal esti-
mates of rotation velocity perpendicular to DOWN, but not
reflected by the angular velocity of DOWN. The latter con-
stant is responsible for the paradoxical discrepancy between
attitude and angular rate sensations predicted by the model.
It was mentioned that the values of these constants are known
only within rather vague limits. They cannot be evaluated
from the data presented in this thesis since they only come
into play when the specific force direction history is incon-
sistent with head attitude history (SF does not remain earth
vertical). They might be illuminated, however, by using the
subjective response tasks developed here during real aircraft
turns.

The data presented here does not allow any distinction
between effects of vestibular and tactile or proprioceptive
cues and must be assumed to represent some unknown combina-
tion of these. As mentioned in Section 2.2., it is also not
clear what the relations between these effects are in the
Ormsby model. It might be interesting to try a similar set
of experiments using a very soft seat designed to distribute
pressure as evenly as possible over the body.

6.5   Implications for Simulation

When subjects experience the Link trainer motion profile
considered most likely, on the basis of the Ormsby model,
to be the optimum simulation of a specific coordinated
turn maneuver, their responses often differ somewhat from
the attitude and angular rate perceptions predicted by the

Ormsby model. These differences have already been discussed
several times and it was concluded that the discrepancy can
probably be explained by viewing it as a threshold detection
problem and considering the workload imposed by the response
task. At least this seems like a far more likely explana-
tion than any of the ready alternatives. If the computer
model used in this thesis represents a signal that is
slightly idealized (no random noise) and simply farther back
along the pathway than the observed output, then it is a use-
ful tool for gauging simulation fidelity. Unfortunately
the experiments performed as part of this thesis are not
sufficient in themselves to unambiguously answer this ques-
tion. If the discrepancies observed are attributable
exclusively to the operation of the assigned response task,
we would expect to get nearly the same attitude estimate
responses if the vertical tracking task is performed in
a real aircraft during a turn similar to the one modeled
in this thesis. The Ormsby model makes the same predic-
tion for altitude perception in both cases and the same
deviation of response output from that prediction should
result. For the case of roll rate perception the model
predicts a different response in the aircraft than in the
simulation. Subject responses to the roll rate magnitude
estimation task in the simulator, however, were often more
like model predictions for aircraft sensations although of
a smaller magnitude. It is therefore not clear what to

expect of responses to this task in the aircraft, but it would be extremely interesting to find out.

A possible approach to such an experiment is to put a subject in an aircraft copilot or passenger seat, outfitted with a hand grip device like the one used in this work, and installed in a similar position with respect to the subject (see Figure 3.10). An IFR training visor or some other method will be necessary to restrict the subject from seeing through the windows or seeing the pilot's instruments. It will be impossible for even a talented pilot to precisely reproduce a specified turn profile, but if an inertial package is used to record the actual motion history (attitude, angular rate, and acceleration) any deviations can be taken into account. Turns can probably be made close enough to the idealized profile of Figure 2.4 to allow meaningful comparisons of subjective vertical tracking task and roll rate estimation data with that presented in this thesis. Ormsby model predictions for both the aircraft and simulation are shown in Figure 2.16 and 2.17. Examples of subjective responses to the predicted optimum simulation profile appear in Figures 5.11, 5.12, 5.21 and 5.22.

Experimental results indicate than an optokinetic display probably will not contribute much to innate sensations of roll motion in a simulator unless, perhaps, the display is of considerably more compelling nature than the moving stripes used in this work. As discussed in Section 6.3, the result is not surprising, considering the short duration of the roll motions

used. This does not imply that the stripe display, or some-
thing similar is not of potential use in simulation. Even if
it does not "fool" a pilot with illusory roll motion, it may
be used as a cue by pilots and contribute to performance. For
instance, Junker and Price [14] have shown that the use of a
display almost identical to the one used here had the same
effect on performance of a difficult visual tracking task as
the introduction of actual roll motion.

The "canned" or predetermined motion profiles used in
the experiments of this thesis were not really designed for
pilot rating of the simulations. Idealization of the turn
profile may have an insignificant effect on perceptual quan-
tities when compared to the effects of coordination (mainten-
ance of the specific force vector in vertical alignment with
respect to the cockpit), but these small differences may
be very important when a pilot is asked to compare his
feelings with those he remembers from real flight. It
should be expected that the idealized version would feel
too mechanical and in fact that was the observation emphasized
by two pilots when asked to evaluate the simulation pro-
files. Pilots can much more reliably evaluate the realism
of a simulation when they can "fly" the simulator as opposed
to being passive observers. It was felt, however, that
while the experiment was in operation there was certainly
nothing to be lost by asking pilots to rate the simulation
profiles using a very simple "realism" scale. The results
do show a definite preference for the profile predicted as
best by perception model considerations, but there were

only three basic choices. There are many alternative
simulation profiles that were not represented. The results
do help verify the conclusion that the stripe display has
little effect on feelings or sensations of motion during the
turn simulation runs. The rating task data can be considered
supportive of conclusions drawn from the Ormsby model, but
for the reasons cited above and because only two pilots
were used the significance of this support must be considered
quite low.

There are two obvious avenues for extension of this
work towards motion simulation applications. One is to
have subjects perform the vertical tracking and roll rate
estimation tasks in an aircraft during the real coordinated
turn maneuver. This would be valuable both for comparison
with model predictions and with subjective results obtained
during various ground based simulations. Data presented
in this thesis should serve as a good data base.

The other obvious extension is to convert the Ormsby
model predictions into a motion logic system for the Link
trainer. The simplest approach is to fit linear dynamics
to Ormsby model predictions of optimum simulator profiles
for some specific maneuvers such as the coordinated turn
discussed in this thesis. If this logic were implemented,
pilots could actually "fly" the trainer and rate the simu-
lation. Such experiments would aid in determining the
validity of the fidelity prediction scheme developed in

section 2.3 and would probably result in refinement or modification of that scheme.

The roll simulation profile suggested as optimum for simulating a coordinated turn on the Link trainer looks much like a high pass filtered version of the real aircraft roll profile. A high pass filter is one of the most common washout devices used in simulator motion logic design and its use would by no means be an innovation. The model does however, suggest parameters for the filter. For instance, the second order filter

$$\phi_{sv}(s) = \left\{ \frac{.5s^2}{(s + .1)(s + 2)} \right\} \phi_{av}(s) \qquad (6.2)$$

$\phi_{sv}(s) \equiv$ Laplace transform of simulator roll

angle $\phi_{sv}(t)$

$\phi_A(s) \equiv$ Laplace transform of aircraft roll angle

$\phi_{av}(t)$

will yield a simulator roll profile similar to the one predicted as optimum when ϕ_{av} follows the idealized aircraft turn profile developed in section 2.1 (see figure 2.4). Figure 6.2 shows a comparison of the two. If this is to be used in an on-line motion logic system so that a pilot can "fly" the simulator as suggested in the last paragraph, non-coordinated situations must be provided for too. Remember that coordination implies a specific force vector that always remains vertical with respect to the cockpit. Although this condition was assumed throughout the idealized turn discussed in Chapter II, a real pilot cannot maintain

roll angle

$3°$

$2°$

$1°$

• simulator roll profile shown, with Ormsby
model, to produce attitude perception closely
matching perception in aircraft

- - - - response of $G(s) = \dfrac{.5s^2}{(s+.1)(s+2)}$ to $10°/sec$
ramp, of 3 seconds duration, beginning at
$t = 3$.

0   1   2   3   4   5   6   8   9   t(sec)

201

Figure 6.2   Comparison of suggested linear simulator roll dynamics and profile found,
with the Ormsby model, to yield attitude perceptions similar to those
felt during an idealized coordinated turn.

perfect coordination. Figure 6.3 suggests a possible roll
axis logic for a three degree of freedom simulator like the
Link trainer. Side force (indicating lack of coordination)
is handled in a more or less traditional manner. Before
the system is implemented it would probably be useful to
run some non-coordinated situations through the model to
check predicted performance of the side force loop. This
can be analysed using the fidelity index program (listed in
Appendix A and described in Section 2.4) in the same way
the coordinated turn situation was analysed in Chapter II,
and should lead to predictions for the best low pass
filter parameters. Figure 6.4 suggests a pitch channel.
The pitch channel is designed to approximate the elevator
illusion based on the non-linear saccule input-output
function hypothesized by Ormsby in Chatper 7 of his thesis
(21). It assumes that aircraft pitch motions will be un-
coordinated. In Figure 6.4, $(\hat{\Theta}_{hd} - \hat{\Theta}'_{hd})$ is the difference
between a given pitch angle in 1 g and at $|\underline{SF}|$ due to
saccule nonlinearity. The low pass filter reflects the fact
that $(\hat{\Theta}_{hd} - \hat{\Theta}'_{hd})$ is felt only by the otoliths, is not con-
firmed by the canals, and therefore is low pass filtered
by the subject's perceptual system (see Figure 2.9). When
this illusion is approximated with simulator pitch motion,
canals will be stimulated also, and the signal will not be
low pass filtered by the subject. If the "aircraft" is

Figure 6.3   Possible roll logic for 3 degree of freedom (θ, ϕ, and ψ)
simulator. Parameters for the high pass filter have been
chosen on the basis of Ormsby model predictions for idealized
coordinated turn (zero side force). Parameters for the low-
pass filter can be chosen by looking at two different side
force conditions with the model, predicting optimums for
each, and balancing between the two. One condition is air-
craft roll with no movement of SF in the inertial frame,
during which we would probably like the l.p. filter to be
one minus the h.p. filter so that everything gets through.
The other condition is side force with no aircraft roll,
during which the optimal l.p. filter may have somewhat slower
dynamics.

θ_{av} (pitch angle of aircraft)

COMPUTE UNIT VECTOR IN DIRECTION OF $\underline{SF}$

$\vec{SF}'_{av}$

COORDINATE TRANSFORMATION TO SENSOR COORDINATES

SF'_{xs}

SF'_{zs}

COMPUTE:
$$\theta = \tan^{-1}\{\frac{SF'_{xs}}{f_{sac}(SF'_{zs})}\}$$

PITCH OF SENSOR COORDINATES WITH RESPECT TO HEAD

$\hat{\theta}'_s$

$\hat{\theta}'_{hd}$

$25°$

$\hat{\theta}_{hd}-\hat{\theta}'_{hd}$

LOW PASS FILTER

$\underline{SF}_{av}$ (g's)

(specific force vector in aircraft vehicle coordinates)

COORDINATE TRANSFORMATION TO SENSOR COORDINATES

SF_{xs}

SF_{zs}

COMPUTE:
$$\theta = \tan^{-1}\{\frac{SF_{xs}}{f_{sac}(SF_{zs})}\}$$

$\hat{\theta}_s$

$\hat{\theta}_{hd}$

θ_{sv} (pitch angle of simulation cockpit)

$$f_{sac}(x) = \{ \begin{array}{l} -0.4x - 1.27, \quad x < -\cos 25° \\ +0.6x - 0.36, \quad x > -\cos 25° \end{array}$$

(f_{sac} is the saccule nonlinearity used in the Ormsby model [21])

Figure 6.4 Possible pitch logic for 3 degree of freedom simulator incorporating elevator illusion.

205

is performing the idealized turn used in this thesis (Figure 2.4) simulator pitch motion will be very close to the profile based on the Ormsby model and used in the experiments (SIM1). Note th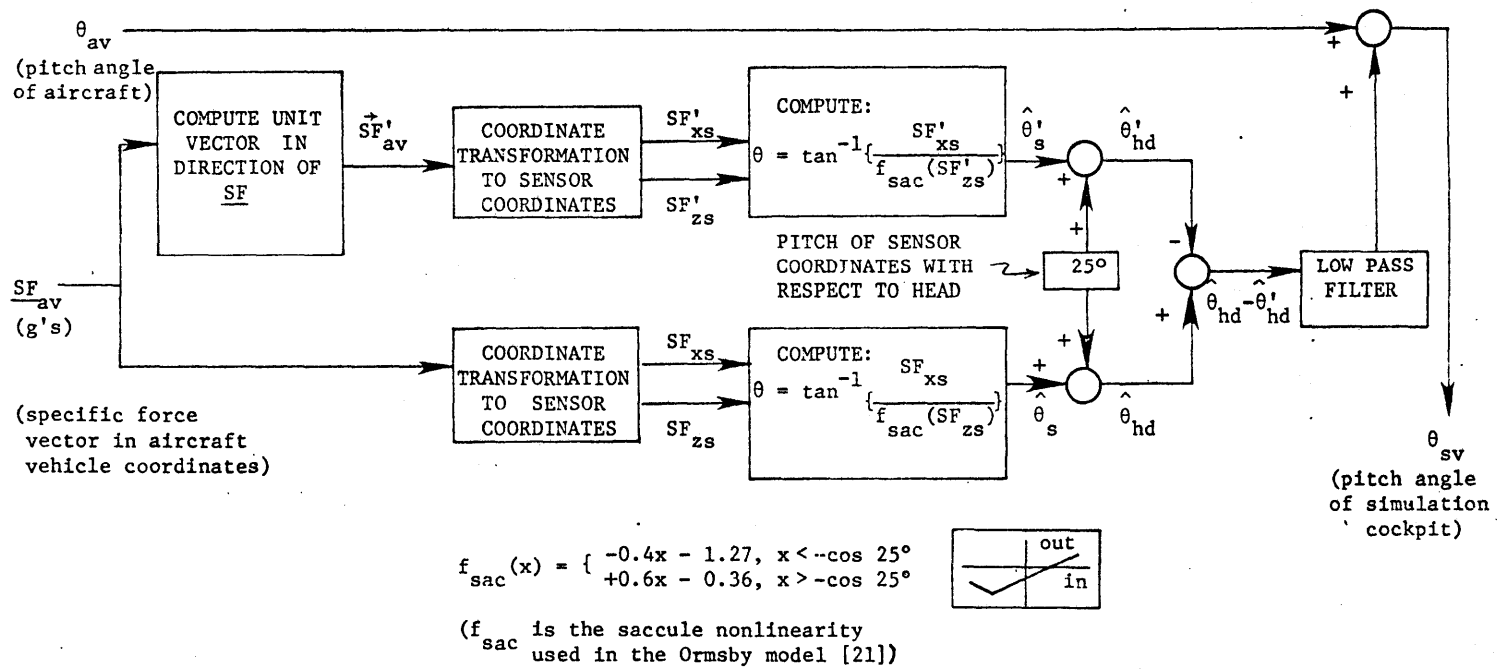at in this case, only the bottom pathway will be non-zero. If coordination in the pitch plane is required, the top channel (θ_{av}) will have to be replaced by something similar to the scheme in Figure 6.3. Yaw can be designed to satisfy

$$r_{sv} = r_{av} \frac{\cos\phi_{av}\cos\theta_{av}}{\cos\phi_{sv}\cos\theta_{sv}} \tag{6.3}$$

This will lead to the same yaw rate component about $\vec{i}_{zhd}$ in both the simulator and imaginary aircraft. It must be emphasized that these suggestions are extrapolations from the specific case analyzed here, and although they are consistent with findings if pilot input produces the same profile assumed in this work for a coordinated turn, they have not yet been tried in a more general sense.

A more sophisticated approach is to design an on-line optimization algorithm for simulator motion employing the perceptual model. This would be especially useful in extending the application of the model to five and six degrees of freedom, but is far beyond the scope of this thesis.

CHAPTER VII

CONCLUSION

7.1   Summary of Results

This thesis begins with the discussion of a specific

aircraft motion profile, an idealized version of the coor-

dinated turn, since this maneuver demonstrates a basic

simulation problem. The problem is that the specific force

vector remains in the X-Z plane even when the aircraft is

banked, a condition that is impossible to achieve in a

three rotational degree of freedom simulator and impossible

to sustain for long periods in almost any ground based sim-

ulator. The problem lends itself to analysis with a physio-

logical motion perception model. Using the Ormsby Human

Dynamic Orientation model [21] as the basic element, a program

was written to compute an index related to the fidelity or

realism of a simulation. The model predicts that a specific

force vector which rolls with the cockpit will produce con-

flicting perceptions of roll angle and roll rate, and the

fidelity analysis implies that a three rotational degree of

freedom simulation should remain faithful to attitude (orien-

tation angle) perception. The fidelity program was used to

predict a coordinated turn simulation profile for a three degree of freedom device most likely to yield the best possible fidelity. The word "fidelity" refers to the degree to which motion sensation in the simulation matches that in the aircraft. Since the model is in the form of a discrete time program that updates the sensors every 0.1 second and updates the optimal estimators every second, there is some degree of approximation inherent in the result.

The Ormsby model considers only non-visual cues. A very simple visual display (a moving stripe roll display) was proposed as a possible means for improving the fidelity of the turn simulation.

The idealized turn profile considered is a 10°/second roll into a 30° bank, 85 knot turn, maintaining constant air speed, constant altitude and perfect coordination. The proposed simulator roll profile looks very much like a second order, high pass filtered version of the aircraft profile, peaking at about 2°. In Chapter VI, parameters are suggested for a second order filter that will probably create a similar match with aircraft perception in terms of the Ormsby model. The simulator pitch profile involves a pitch up motion during roll in, a pitch up angle of about 4° sustained throughout the steady turn, and a pitch down to zero during roll out. Yaw is simply adjusted to provide the same component about the head vertical axis as in the aircraft.

A series of experiments were devised in order to judge
the effectiveness of two open loop, subjective, perception
indication tasks; and to apply these towards checking model
predictions and visual display effects in our modified Link
GAT-1 trainer. One task is that of keeping a long pointer
aligned with perceived earth vertical. The pointer is fixed
to a handgrip device that has rotational freedom about the
pitch and roll axes and is instrumented to provide a remote
readoff of pitch and roll angle. The other task consists of
continuously estimating subjective roll velocity proportional
to a modulus or standard, and continuously outputting this
estimate on a voltmeter scale. The meter needle can be con-
trolled with the same handgrip device used in the first task.

Results from five subjects show that people are fairly
self-consistent in both tasks and exhibit a high degree of
correlation between stimulus and response. In the rate
estimation task, there was great consistency among subjects
as well, and people responded with a near one to one ratio
between peak stimulus and peak response. This proportional
scaling law may reflect the design of the response scale,
range of stimulus used, and selection of the modulus. It
may also represent a small, approximately linear, segment
of some other function. Log and power law functions are
far more commonly found in psychological scaling experiments,
but the relationship found here is very convenient and in-
creases the usefulness of the task.

The vertical tracking task results varied somewhat from subject to subject ranging from consistent underestimation of roll or pitch angle by about 50% to consistent overestimation by about 100%. There is no trend towards better roll than pitch performance or vice versa, and most subjects were able to track simultaneous pitch and roll motions as well as one or the other alone. If work load is increased, this may no longer be the case. Since the subjects tend to be self-consistent and are able to track pitch and roll simultaneously, the two axis vertical tracking task is certainly of potential use in measuring subjective attitude perception.

Usefulness of both tasks seems to be restricted to low frequencies, which should be expected from open loop estimation procedures. Consideration of response lags in the data suggest a maximum effective bandwidth of 0.25 Hz, but since the stimuli used in the experiments were predominantly of lower frequency, this must be considered a very rough estimate.

Application of the coordinated turn simulation profile discussed before leads to unexpected results. Instead of following the roughly trapezoidal roll profile (from zero to 2° and back to zero during roll in and roll out phases of the turn), responses to both tasks often indicated only the initial leg of the trapezoid, almost as if the stimulus were being integrated. When the magnitude of the roll profile was multiplied by 2, the same phenomenon was observed occasionally, but more often the expected result was achieved. Roll profiles

that were simply attenuated versions of the aircraft roll profile (simulator rolled 5° during roll in, remained there for the constant rate turn, and returned to zero during roll out), produced the expected results; responses followed the stimulus. The deviation from predicted response can probably be explained by the response lag inherent in the task plus consideration of the dynamic detection threshold effects, but this obviously needs further investigation. The pitch elevator illusion was always felt and indicated as expected.

The attempt to improve the simulation fidelity with an optokinetic roll display was not successful. In fact, the display showed no large significant effects during any combination with cockpit roll motion. This result is not surprising considering the short durations of the roll motion, the relatively long onset time usually associated with circularvection and the otolith contribution in the vertical plane. It is possible that a very small enhancement of the roll rate sensation was created when the display was counterrolled at four times the simulator roll rate during very low roll rate (<3°/sec) stimuli. Possibly gains higher than 4 will produce larger significant effects. It seems unlikely that this type of roll display can be used to make sensations of motion more realistic in simulators unless, perhaps, it is of a considerably more compelling nature than ours (perspective displays, realistic scene displays, etc). This does not mean that the roll stripe display will not affect the pilot's

performance in a simulator. Any cues provided by the stripes will probably be utilized whether or not the pilot is "fooled" into feeling illusory motion sensations.

Neither the idealized coordinated turn profile nor the canned simulation profiles used in the experiments were originally intended as part of a pilot rating scheme. However, two pilots were asked to imagine themselves as passengers during a 30° bank, 85 knot, constant altitude coordinated turn, and to rate the "realism" of the maneuver. Of the three motion profiles used, the profile predicted as best received the highest ratings, the proportional roll strategy recieved the lowest and the stripe motion profile did not produce any consistent preference. All simulations were felt to be too mechanical.

A far more effective way to obtain reliable pilot ratings of a simulation is to create a setup in which pilots can "fly" the simulator. A dynamic motion logic was proposed as a first attempt at a scheme that will "fly" like the simulation profile suggested by the Ormsby model, during coordinated turn maneuvers.

7.2   Concluding Remarks

The questions posed in the introduction have been answered in part, although many uncertainties remain. The effectiveness and limitations of the perception indication

tasks have been considerably illuminated. The potential for the stripe display has also been more clearly defined. Some of the data collected supports the Ormsby model predictions; in some instances it is too noisy for a meaningful comparison; and in one case, while not clearly contradicting the model predictions, the results need further explanation. The pilot "realism" evaluations provide some extremely weak support for the fidelity prediction scheme, but the scheme cannot be evaluated in a meaningful way without perceptual data during aircraft flights and pilot evaluation of a simulator they can "fly". The results presented in this thesis provide an essential data base for the former, since the ground based and flight tests are most meaningful by comparison.

7.3   Suggestions for Further Research

Results discussed in the thesis can be extended and clarified by further work in the following areas:

1.   It would be extremely useful to have data indicating attitude and roll rate perceptions in real aircraft during coordinated turns with known attitude and acceleration profiles. Such data could be compared directly to ground based results and would help determine precisely how perceptions during various simulations differ

from those in the aircraft. It would also be of help in evaluating model predictions for this maneuver.

2.   Predictions for optimum fidelity simulation profiles should be implemented as on-line motion logic systems so that simulators can be "flown" and evaluated by pilots. This is the only effective way to gauge the validity of the fidelity prediction scheme and to improve or revise the scheme. In addition, the type of cost analysis described in Chapter II should be extended to incorporate a mathematical minimization procedure that can be applied to more general cases. Analysis can also be expanded to 5 and 6 degree of freedom simulators. An eventual goal might be an on-line optimization routine based on the physiological model to be included in simulator motion systems.

3.   Finally, as more data becomes available, it should be incorporated into expanded models that attempt to differentiate between vestibular and tactile stimuli as well as models that account for visual cues.

NOTE: The appendices containing programming
         material are contained in Volume II
         of this Thesis.

REFERENCES

1. Affifi, A.A. and Azen, S.P. *Statistical Analysis: A Computer Oriented Approach*, New York: Academic Press, 1974.

2. Berthoz, A., Pavard, B., and Young, L.R. "Perception of linear horizontal self-motion induced by peripheral vision (linearvection): Basic characteristics and visual vestibular interactions", *Experimental Brain Research* 23:471-489, 1975.

3. Brandt, T., Dichgans, J., and Koenig, E. "Differential effects of central versus peripheral vision of egocentric and exocentric motor perception", *Experimental Brain Research* 16:476-491, 1973.

4. Clark, B. "Thresholds for the perception of angular acceleration in man", *Aerospace Medicine* 38:443, 1967.

5. Clark, B. and Stewart, J. "Thresholds for perception of angular acceleration about the three major body axes" Fourth Symposium on the Role of the Vestibular Organs in Space Exploration, NASA SP-187, 1968.

6. Clark, B. and Stewart, J. "Effects of angular acceleration on man: Thresholds for the perception of rotation and oculogyral illusion", *Aerospace Medicine* 40, 1969.

7. Conrad, B. and Schmidt, S.F. "A study of techniques for calculating motion drive signals for flight simulators", NASA CR-114345, July 1971.

8.   Conrad, B., Schmidt, S.F. and Douvillier, J.G. "Washout circuit desing for multi-degree-of-freedom moving base simulators", AIAA Paper No. 73-929, AIAA Visual and Motion Simulation Conference, Palo Alto, California, September 10-12, 1973.

9.   Dichgans, J., Diener, H.C. and Brandt, T. "Optokinetic graviceptive interaction in different head positions", *Acta Otolaryngol* 78:371-398, 1974.

10.   Dichgans, J., Held, R., Young, L.R., and Brandt, T. "Moving visual scenes influence the apparent direction of gravity", *Science* 178:1217-1219, 1972.

11.   Gai, E. Psychophysical Models for Signal Detection with Time Varying Uncertainty, Ph.D. Thesis, Department of Aeronautics and Astronautics, Massachusetts Institute of Technology, 1975.

12.   Groen, J.J., and Jongkees, L.B.W. "The threshold of angular acceleration perception", *J Physiol* 107:1-7, 1948.

13.   Howard, I.P. and Templeton, W.B. Human Spatial Orientation, New York: John Wiley and Sons, 1966.

14.   Junker, A.M., and Price, D. "Comparison between a peripheral display and motion information on human tracking about the roll axis. AIAA Visual and Motion Simulation Conference, Dayton, Ohio, April 26-28, 1976.

15. Kornhuber, H.H. (Ed.) <u>Handbook of Sensory Physiology.</u> <u>Vestibular System. Part I.   Basic Mechanisms</u>, New York: Springer-Verlag, 1974.

16. Kuethe, A.M. and Schetzer, J.D. <u>Foundations of Aero-</u> <u>dynamics</u>, New York: John Wiley and Sons, 1959.

17. Lichtenstein, J.H. and Saucer, R.T. "Experimental investigation of the visual field dependency in the erect and supine positions", NASA TN D-6883, 1972.

18. Meiry, J.L.   <u>The Vestibular System and Human Dynamic</u> <u>Space Orientation</u>, Sc.D. Thesis, Department of Aero- nautics and Astronautics, Massachusetts Institute of Technology, 1965.

19. Murphy, R.E.   <u>A Display System to Induce Self Rotation</u>, S.M. Thesis, Department of Aeronautics and Astronautics, Massachusetts Institute of Technology, 1972.

20. Oosterveld, W.J. "Threshold values for stimulation of the horizontal semicircular canals", *Aerospace Medicine* <u>14</u>:386, 1970.

21. Ormsby, C.C. <u>Model of Human Dynamic Orientation</u>, Ph.D. Thesis, Department of Aeronautics and Astronautics, Massachusetts Institute of Technology, 1974.

22. Parrish, R.V., Dieridonne, J.E., Bowles, R.L. and Martin, D.J. "Coordinated adaptive washout for motion simulators" AIAA Paper No. 73-930, AIAA Visual and Motion Simulation Conference, Palo Alto, California, September 10-12, 1973.

23. Parrish, R.V. and Martin, D.J. "Evaluation of a linear washout for simulation motion cue presentation during landing approach", NASA TN D-8036, 1975.

24. Poulton, E.C. "The new psychophysics: Six models for magnitude estimation", *Psychological Bulletin* 69:1-19, 1968.

25. Schmidt, S.F. and Conrad, B. "Motion drive simulator signals for piloted flight simulators", NASA CR-1601, May, 1970.

26. Sinacori, J.B. "A practical approach to motion simulation", AIAA Paper No. 73-931, AIAA Visual and Motion Conference, Palo Alto, California, September 10-12, 1973.

27. Snedecor, G.W. and Cochran, W.G. Statistical Methods Ames, Ohio: The Iowa State University Press, 1969.

28. Stevens, S.S. "On the operation known as judgement", *American Scientist* 54:385, 1966.

29. Taylor, J.W.R. (Ed.) Jane's All the World's Aircraft 1975-1976, New York: Franklin Watts, Inc., 1975.

30. Van Houtte, N.A.J. Display Instrumentation for V/STOL Aircraft Landing, Sc.D. Thesis, Department of Aeronautics and Astronautics, Massachusetts Institute of Technology, 1970.

31. Witkin, H.A. and Asch, S.R. "Studies in space orientation. Further experiments on perception of the upright with displaced visual fields", *J Exp Psychol* 38:762-782, 1948.

32.   Young, L.R. "Role of the Vestibular System in Posture
       and Movement", In: Medical Physiology, V.B. Mountcastle
       (Ed.), 13th Edition, Volume I, Chapter 27. Saint Louis:
       C.V. Mosby and Co., 1974.

33.   Young, L.R., Dichgans, J., Murphy, R. and Brandt, T.
       "Interaction of optokinetic and vestibular stimuli in
       motion perception", *Acta Otolaryngol*   76:24-31, 1973.

34.   Young, L.R., Oman, C.M. and Curry, R.E. "A descriptive
       model of multisensor human spatial orientation with
       applications to visually induced sensations of motion"
       AIAA Paper No. 73-915, AIAA Visual and Motion Simulation
       Conference, Palo Alto, California, September 10-12, 1973.

35.   Young, L.R., Oman, C.M. and Dichgans, J. "Influence of
       head orientation on visually induced pitch and roll
       sensations", *Aerospace Medicine* 46:264-268, 1975.

36.   Young, L.R. and Meiry, J. "A revised dynamic otolith
       model", *Aerospace Medicine* 39:606-608, 1969.

37.   Salih, W.A. Design, Construction and Testing of a
       Manual Orientation Indicator, E.A.A. Thesis, Department
       of Aeronautics and Astronautics, Massachusetts Institute
       of Technology, 1974.